THEORETICAL SOLUTIONS FOR THE JET FLAP DIFFUSER

Thesis by

Jean-Pierre G. Morel

In Partial Fulfillment of the Requirements

For the Degree of

Aeronautical Engineer

California Institute of Technology

Pasadena, California

1969

(Submitted May 28, 1969)

ACKNOWLEDGMENTS

The author would like to express his appreciation to Dr. Peter Lissaman for his encouragement and guidance during this study and to the GALCIT for providing financial assistance. Special indebtedness is owed to Dr. Gordon Harris for his friendship and for his helpful advice.

The drawings were prepared by Mrs. Betty Wood, whose patience is much appreciated. Sincere gratitude is owed to Mrs. Elizabeth Fox for help throughout the typing and in the preparation of the manuscript.

ABSTRACT

This study proposes a jet sheet as an alternative to a rigid diffuser for a momentum propulsor. This appears attractive technically. The diffuser shape can be tailored by modulating jet momentum and angle and can be switched off in forward flight since its main function is increasing thrust/power ratio at static speeds. Theoretical analysis for a steady inviscid incompressible flow predicts impressive thrust augmentations. Taking into account the energy required to feed the jet sheet, it appears that in some cases propulsor thrust can be more than doubled. It could be applied to ducted fans, jet engines and seems particularly attractive for ejector thrust systems.

A first approach of the study of the flow is made in the planar and axisymmetric cases by assuming that the velocity is uniform in each section. For the planar problem a linearized solution is presented. A conformal mapping transforms it into a half-plane boundary value problem of the Riemann-Hilbert-Poincaré type. It is solved by combining Hilbert Transforms, asymptotic expansion and a digital computer program. Then the nonlinear two-dimensional problem is presented with some references to the way it could be solved.

TABLE OF CONTENTS

PART	TITLE	PAGE
	ACKNOWLEDGMENTS	ii
	ABSTRACT	iii
	TABLE OF CONTENTS	iv
	LIST OF FIGURES	vi
	LIST OF SYMBOLS	viii
I	INTRODUCTION	1
II	GLOBAL APPROACH	4
	1. Simple Momentum Analysis for Planar and Axisymmetric Flows	4
	2. Application to Shrouded Propeller	8
	3. Application to Ejector	10
III	ANALYSIS OF THE FLOW	16
	1. Physical Problem: Qualitative Analysis of the Flow Field	16
	2. One-Dimensional Planar and Axisymmetric Analysis	20
	3. Two-Dimensional Potential Analysis	23
	A. Physical Problem	23
	B. Conformal Mapping - Asymptotic Expansions of $\overline{V}$ as $X \rightarrow 0$ and $X \rightarrow 1$	25
	C. Method of Solution: Mathematical Problem	28
	D. Results: Comparison between One-Dimensional and Planar Theory	30
	4. Nonlinear Two-Dimensional Problem	32
	A. Formulation of the Problem	32

TABLE OF CONTENTS (Cont'd)

PART	TITLE	PAGE
	B. Approximate Method of Solution for the Linear Two-Dimensional Problem	36
IV	SUMMARY AND CONCLUSIONS	41
	REFERENCES	43
	APPENDIX	45
	FIGURES	50

LIST OF FIGURES

FIGURE NO.		PAGE
1	Thrust Performance of Static Propulsion System	50
2	Geometry of Jet Flap Diffuser	51
3	Diffusion Coefficient for Planar or Axisymmetric Flow	52
4	Amplification for Given Total Head Flow	53
5	Amplification for Given Total Power Flow with Fixed Jet Thickness	54
6	Amplification for Given Total Power Flow with Varying Jet Thickness	55
7	Comparison of Jet Flap Diffuser with Conventional Actuator System	56
8	Comparison of Jet Flap Diffuser with Conventional Ejector System	57
9	Comparison of Jet Flap Diffuser/Ejector with Jet Engine (Fixed Jet Speed)	58
10	Comparison of Jet Flap Diffuser/Ejector with Jet Engine (Fixed Power)	59
11	Comparison of Jet Flap Diffuser/Ejector with Ejector (Fixed Power)	60
12	Performance of Jet Flap Diffuser on Specific Jet Engine	61

LIST OF FIGURES (Cont'd)

FIGURE NO.		PAGE
13	Geometry in the Physical Plane	62
14	Linearized Geometry	63
15	V Component in Auxiliary Plane	64
16	U and V Component in Auxiliary Plane	65
17	Solution in Physical Plane	66
18	Geometry of Nonlinear Planar Problem	67
19	Geometry in the Potential Plane	68
20	Regions of the Nonlinear Problem	69
21	Auxiliary Planes for the Nonlinear Problem	70

LIST OF SYMBOLS

D	Half width (2. D.) or radius (Ax.) of the internal flow in the infinite downstream section
Ho	Total head in the internal flow
He	Total head in the external jet
$\dot{I}e$	Impulse of the external jet
P	Total required power
S	Area of a flow
S_1	Area of the internal flow in the duct
S_2	Area of the internal flow in the infinite downstream section
T	Thrust
V_e	Velocity of the external jet
ℓ	Half width (2. D.) or radius (Ax.) of the duct
p_o	Ambient pressure
s	Thickness of the jet sheet at the exit from the duct
x, y	Rectangular coordinates with x along the center-line
α	Angle of the jet sheet at its exit from the duct with respect to the center-line
$\delta = \frac{s}{\ell}$	Thickness ratio of the jet sheet
ρ	Density of the fluid
σ	Two-dimensional flow: $\sigma = D/\ell$ Axisymmetric flow: $\sigma = D^2/\ell^2$

Symbols for the Momentum Analysis: Planar and Axisymmetric Flows (II. 1)

$[A]_{Ho}$	Thrust amplification for given total head flow
$[A]_P$	Thrust amplification for given total power flow

LIST OF SYMBOLS (Cont'd)

C_J External jet momentum coefficients: two-dimensional flow:

$$C_J = \frac{\rho s V_e^2}{\frac{\rho}{2} \ell V_o^2}$$

axisymmetric flow: $C_J = \frac{2\pi \ell s \ell V_e^2}{\pi \ell^2 \frac{\rho}{2} V_o^2}$

H_o^* Total head of the internal flow without jet flap diffuser

P_J Total power required by the jet flap diffuser system

P_o^* Total power required by the internal flow without jet flap diffuser

T_J Thrust of the jet flap diffuser system

T_o^* Thrust of the internal flow without jet flap diffuser

V_o Velocity of the internal flow in the infinite downstream section

V_1 Velocity of the internal flow in the infinite upstream section

V_o^* Velocity of the internal flow without jet flap diffuser

p_1 Static pressure of the internal flow in the infinite upstream section

Symbols for the Application to Shrouded Propeller (II. 2)

P_1 Total power required by a plain propeller

P_2 Total power required by a ducted propeller

P_3 Total power required by a ducted propeller - jet flap diffuser system

S Area of the propeller disk

T_1 Thrust of a plain propeller

LIST OF SYMBOLS (Cont'd)

T_2 Thrust of a ducted propeller

T_3 Thrust of a ducted propeller - jet flap diffuser system

V_1 Velocity in an infinite downstream section of the flow due to a plain propeller

V_2 Velocity in an infinite downstream section of the flow due to a ducted propeller

V_3 Velocity in an infinite downstream section of the internal flow due to a ducted propeller with jet flap diffuser

Symbols for the Application to Ejector (II. 3)

A Ejector parameter: two-dimensional flow $A = a/\ell$

axisymmetric flow $A = a^2/\ell^2$

C_J External jet momentum coefficient: two-dimensional flow

$$C_J = \frac{\rho s V_e^2}{\rho a V_J^2}$$

axisymmetric flow $C_J = \dfrac{2\pi\rho s \ell V_e^2}{\pi a^2 V_J^2}$

$\dot{I}$ Thrust amplification of jet flap diffuser on specific jet engine

P_1 Total power required by a plain jet

P_2 Total power required by an ejector

P_3 Total power required by an ejector - jet flap diffuser system

S Area of the plain jet

T_1 Thrust of the plain jet

T_2 Thrust of the ejector

T_3 Thrust of the ejector - jet flap diffuser system

T_J Thrust of the jet engine

LIST OF SYMBOLS (Cont'd)

T_e Thrust of the jet sheet

T Thrust of the jet engine without bleeding

V_1 Velocity in an infinite downstream section of the flow due to a plain jet

V_2 Velocity in an infinite downstream section of the flow due to an ejector

V_3 Velocity in an infinite downstream section of the internal flow due to an ejector - jet flap diffuser system

V_S Velocity of the induced flow in the plane of the jet engine

V_i Velocity of the internal flow at the exit of the mixing chamber

V_J Velocity at the exit of the jet engine in the ejector configuration

V_J^* Velocity at the exit of the jet engine (alone)

a Half width (2. D.) or radius (Ax.) of the exit of the jet engine

p_S Static pressure in the plane of the jet engine

p_i Static pressure at the exit of the mixing chamber

Symbols for the Analysis of the Flow (III)

C_J External jet momentum coefficient:

Two-dimensional flow $C_J = \dfrac{\rho s V_e^2}{\frac{\rho}{2} \ell V_o^2}$

Axisymmetric flow $C_J = \dfrac{2\pi\rho s \ell V_e^2}{\pi \ell^2 \frac{\rho}{2} V_o^2}$

C_p Pressure coefficient, $C_p = \dfrac{p-p_o}{\frac{\rho}{2} V_o^2}$

LIST OF SYMBOLS (Cont'd)

$\overline{F}$	Complex potential $\overline{F} = \overline{\phi} + i\overline{\psi}$
R	Radius of curvature
$U = \frac{\overline{u}}{a}$	(Two-dimensional potential analysis)
$V = \frac{\overline{v}}{a}$	
V_1	Velocity of the internal flow in the infinite upstream section
X, Y	Rectangular coordinates in the auxiliary plane
$Z = X+iY$	
$h(x)$	Analytic function representing the jet sheet
$p(x, y)$	Static pressure at a point of the physical plane
$p(\tilde{\phi}, \tilde{\psi})$	Static pressure at a point of the $\tilde{\phi}$-$\tilde{\psi}$ plane
$u(x, y)$	Component of the velocity along $\vec{ox}$
$u(h) = u(x, h)$	
$u(0) = u(x, 0)$	
$\overline{u} = \frac{u}{V_1} - 1$	
$v(x, y)$	Component of the velocity along $\vec{oy}$
u_i, v_i	Solution in the physical plane x/ℓ, y/ℓ
u_{ii}, v_{ii}	Solution in the $\overline{\phi}$ - $\overline{\psi}$ plane
$y/\ell\,(x/\ell)$	Nondimensional analytic function representing the jet sheet
$\tilde{w}$	$\tilde{\phi} + i\tilde{\psi}$
$\vec{n}$	Unit vector normal to the boundary
$\vec{t}$	Unit vector tangent to the boundary
ϕ	Velocity potential
$\overline{\phi} = \frac{\phi}{\ell V_1}$	
$\tilde{\phi} = \frac{\phi}{DV_o}$	

LIST OF SYMBOLS (Cont'd)

ψ Stream function

$\overline{\psi} = \frac{\psi}{\ell V_1}$

$\tilde{\psi} = \frac{\psi}{DV_o}$

$\Gamma(\tilde{w}) = \log(\frac{d\tilde{w}}{d\tilde{z}}) = Q(\tilde{\phi}, \tilde{\psi}) - i\theta(\tilde{\phi} - \tilde{\psi})$

θ Deflection of the velocity

Subscripts: i properties of the internal flow

e properties of the external jet

I. INTRODUCTION

The thrust performance of static propulsion systems is measured in terms of the thrust to power ratio (T/P), which, regardless of the details of the particular device employed depends on the effective disc loading T/S as shown in Figure 1.

For high thrust power ratios the disc loading should be small. This can be achieved by expanding the stream tube by means of a rigid diffuser shroud. As is well known, the diffuser angle is limited by flow separation and there may be other practical difficulties of weight and complexity. In addition, the shroud becomes a drag-producing element when the propulsor is in flight and it would be desirable to remove it at high speeds.

A new approach to this is to replace the solid diffuser by a high energy air sheet--this is called the jet flap diffuser. Substantial thrust augmentation can be achieved by this device (even taking into account the energy required to feed the jet sheet). In addition, the thrust can be readily modulated in direction and magnitude simply by varying the jet flap strength or angle. Thus one has, in effect, a continuously varying diffuser of zero weight. An additional advantage is that because there is no solid wall, large diffusion rates can be achieved without boundary layer separation. (Figure 2).

Thus the jet flap diffuser concept has important implications for V/STOL application, both for propulsion and control. This device has been mentioned by Société Bertin & Cie (France) which has made an application for a U. S. patent (N. 2, 922, 277). This company plans to design a jet flap diffuser at the exit of a shrouded propeller,

but no basic research has been done on the project. In cooperation with Nord-Aviation they have developed a "solid blown diffuser" at the exit of a shrouded propeller to prevent flow separation (Ref. 1).

In the United States Chaplin has submitted a patent application (No. 2,998,700) and has made a global momentum analysis which gives the same results as the one presented here in Part II. 1. Chaplin states that this device seems to have high potential of providing a simple and powerful technique for modulation of fluid flow within or at the exit of a duct.

Hazen at Princeton University has referred to flow visualization tests with a jet flap diffuser on a shrouded propeller model in a water tunnel. Some interesting phenomena were observed involving reverse flow at the center of the slipstream, attributed to the wake from the propeller centerbody, when the rate of diffusion was too rapid.

No detailed two-dimensional theoretical analyses of the problem are known, although Luu (Ref. 2) presents a linearized approach to the problem using rheoelectric analog for axisymmetric and planar flows. He considers the two cases of the "regular blowing" (where the jet is tangent to the shroud at its exit) and of the "singular blowing" (where there exists a finite angle between the wall of the shroud at its exit and the jet) and solves using the analog. The results report only the diffusion coefficient, and do not give any other details of the flow.

It is clear that the formulation of the problem is complicated by having a boundary of unknown shape, the jet sheet. The local

pressure difference dictates the curvature of the sheet, while the entire shape of the sheet in turn controls the pressure distribution. To analyze this device the flow is assumed to be both incompressible and irrotational, and the momentum of the jet sheet is assumed constant implying that the jet is of very much higher total head than the rest of the flow and is discharged as a vanishingly thin sheet. The assumptions pertaining to the jet sheet are discussed in detail and substantiated by Spence (Ref. 3).

The purpose of the present investigation is first to give an idea of the applications of such devices and their efficiency, by means of global and momentum analysis; then to study the flow in more detail using appropriate assumptions to permit more complete solutions of the velocity distribution. Two different solutions are given, the one-dimensional approach in which it is assumed that the v flow components are vanishingly small (channel flow), and the linearized two-dimensional approach in which it is assumed that both the u, v perturbation velocities are quite small (planar Laplace flow).

II. GLOBAL APPROACH

In this section the performance of a jet flap diffuser as a thrust augmenting device is analyzed on the basis of global momentum considerations. The results obtained are then applied to determine the performance of shrouded propellers and ejectors equipped with jet flap diffusers.

1. Momentum Analysis for Planar and Axisymmetric Flows

For this approach, we start with two-dimensional flow in the jet flap diffuser as is shown in Figure 2. The flow inside the semi-infinite duct of width 2ℓ is expanded to the ambient pressure p_o. It is assumed that the velocity profiles in the far upstream and downstream sections are uniform, and have magnitudes V_1 and V_o respectively.

The curvature of the jet sheet is directly related to the pressure difference across it. The internal flow is initially at subatmospheric pressure and expands or diffuses to ambient pressure.

To normalize the results, consider the following parameters, the diffusion coefficient $\sigma = D/\ell$, which is the ratio of the area of the main flow in its infinite downstream section to the one of the duct, and the external jet momentum coefficient $C_J = \frac{I_e}{\frac{\rho}{2}\ell V_o^2}$, which is the ratio of the impulse in the jet sheet (which is assumed to be constant along it) to the product of the dynamic pressure of the completely diffused flow and the characteristic diffuser width.

Consider first the two-dimensional case. Then the conservation of momentum along the $\vec{ox}$ axis, the Bernoulli and continuity equations, give the following system of equations:

$$\sigma(p_0 + \rho V_0^2) - (p_1 + \rho V_1^2) = \frac{\rho}{2} V_0^2 C_J (1-\cos\alpha)$$

if $$C_J = \frac{\rho s V_e^2}{\frac{\rho}{2} \ell V_0^2}$$

$$p_0 + \frac{\rho}{2} V_0^2 = p_1 + \frac{\rho}{2} V_1^2$$

$$\sigma = \frac{V_1}{V_0} = \frac{D}{\ell}$$

Its solution gives the diffusion coefficient

$$\sigma = 1 + \sqrt{C_J(1-\cos\alpha)}$$

The total thrust of this jet flap diffuser is:

$$T_J = \rho D V_0^2 + \rho s V_e^2$$

and the total required power

$$P_J = \frac{\rho}{2} D V_0^3 + \frac{\rho}{2} s V_e^3 .$$

Now for zero blowing, one gets for the thrust: if $H_0^* = p_0 + \frac{\rho}{2} V_0^{*2}$

$$T_0^* = \rho \ell V_0^{*2}$$

and for the power required

$$P_0^* = \frac{\rho}{2} \ell V_0^{*3}.$$

Now consider the case when $V_0 = V_0^*$. This could occur when one had such a powerful blower system that it was capable of

providing flow at a given total head regardless of the jet flow requirements. Then the thrust augmentation for a constant total head $[A]_{Ho}$ is:

$$[A]_{Ho} = \left[\frac{T_J}{T_0}\right]_{V_0=V_0^*} = \sigma + \frac{C_J}{2}$$

This coefficient is the thrust augmentation factor attributable to the jet flap diffuser with no consideration given to total available power.

If one considers a power limited system and computes the augmentation for a given power level $P_j = P_0$ one gets the augmentation at constant total* power $[A]_P$ if $V = V_e/V_0$:

$$[A]_P = \left[\frac{T_J}{T_0^*}\right]_{P_J=P_0^*} = \frac{\sigma + \delta V^2}{[\sigma+\delta V^3]^{2/3}}$$

where δ is the ratio of the jet sheet width to half the width of the duct. This coefficient is the thrust augmentation factor achieved by the jet flap diffuser system when total power available is fixed.

For the axisymmetrical case, which is of practical interest in propulsion devices, the nondimensional equations and results are the same if one takes $C_J = \frac{2\pi\rho\ell s V_e^2}{\rho/2\pi\ell^2 V_0^2}$ where s is the thickness of the external jet at x = 0, and $\sigma = D^2/\ell^2$. So for the same performance, in the axisymmetric case, the width of the external jet must be half that used in the plane case. This result is important from a design point of view as usually the actuators are axisymmetrical. Then there is no need to have as thick a jet as in the planar case so the solid wall of the shroud can be thinner, which may be desirable in flight from a drag point of view.

---

* total power = jet flap power + primary flow power

Figure 3 shows the diffusion coefficient σ for different values of C_J and α. From the previous equation, the thrust amplification for a constant total head flow supply $[A]_{Ho}$ is linearly dependent on σ and C_J. Then it is noted on Figure 4 that the total thrust is substantially increased by the jet flap diffuser; this may be of the order of 10.

Figure 5 shows the coefficient of amplification for constant total power, for different values of C_J, α. It is noted that peak thrust augmentation is achieved at small values of C_J. There is no need to develop a high momentum external jet but it is advantageous to have a thick jet as shown in Figure 6, since it is more economical from the power point of view to achieve a given momentum level with a jet of large mass flow and low velocity.

2. Application to Shrouded Propeller

Interest in the shrouded propeller has been stimulated by the need for high static thrust propulsion systems on V/STOL aircraft, ground effect machines and other moderate speed vertical lift vehicles with stringent space limitations. Theoretically, the presence of the shroud substantially reduces the slipstream contraction of the conventional propeller, increasing the mass flow through the propeller disc. These effects may be increased with larger exit to propeller area ratios. This can be obtained by adding a rigid diffuser to the shroud, but we have observed that this solution presents a lot of disadvantages. A better scheme is to use a jet flap diffuser (Figure 7) as shown by the following calculations.

For a free air propeller of area S the slipstream contraction reduces the section of the jet to S/2. Then the thrust and required power are

$$T_1 = \rho \frac{S}{2} V_1^2 \qquad \text{and} \qquad P_1 = \frac{\rho}{2} \frac{S}{2} V_1^3 \quad .$$

For a shrouded propeller of the same area S there is no slipstream contraction and

$$T_2 = \rho S V_2^2 \qquad P_2 = \frac{\rho}{2} S V_2^3$$

For a shrouded propeller supplied with a jet flap diffuser of diffusion coefficient σ we get

$$T_3 = \rho S V_3^2 \left(\sigma + \frac{C_J}{2}\right) \qquad P_3 = \frac{\rho}{2} S V_3^3 \left(\sigma + \frac{C_J}{2} \frac{V_e}{V_3}\right)$$

Assuming that the total power used is the same, $P_1 = P_2 = P_3$, figure 7 shows the order of augmentation of thrust achieved by use of the jet

flap diffuser. These results give only some idea of the gain of thrust which could be obtained.

No experimental data have been found on a real jet flap diffuser, but one can mention the experimental results obtained by Societes Bertin and Nord-Aviation (Ref. 1) on a shrouded propeller. The addition of a blown diffuser of 45^{o} (half-angle) and also the blowing of the rear part of the centerbody gives at least an increase of 18% of thrust for a total given power. We observe that this figure is in the range of what is predicted by this simple theoretical approach.

3. Application to Ejector

The prospect of exploiting the principle of ejector thrust augmentation has been gaining interest in the field of V/STOL aircraft development and rocketry. For example, Reference 4 presents the wind tunnel tests of a variable ejector nozzle with an aerodynamically positioned shroud at Mach numbers from 0 to 2.0 at simulated power settings for supersonic cruise, subsonic cruise, reheat acceleration, dry acceleration and idle descent. This nozzle had typically high efficiencies at supersonic cruise and reheat acceleration conditions but rather low performance at subsonic cruise and dry acceleration conditions. Unhappily no information is given on the relative performance of this variable ejector nozzle, as no test has been done without this improving device.

Consider the generalized ejector configuration shown in Figure 8 where a jet sheet of velocity V_J is issued from a nozzle and discharged into a mixing chamber formed by the shrouds. As the jet expands to fill the mixing chamber, it entrains fluid from the originally quiescent surroundings, thereby inducing a secondary flow into the ejector. This induced flow gives substantial thrust augmentation. A way to amplify this secondary flow is to add a jet flap diffuser at the exit of the mixing chamber. In this way major augmentation of thrust may be achieved as is shown by the following calculation.

For a free-air jet engine (Figure 8) the thrust and required power are:

$$T_1 = \rho S V_1^2 \qquad P_1 = \frac{\rho}{2} S V_1^3$$

For a two-dimensional ejector the basic application of the momentum and Bernoulli theorems gives the three following relations

$$\rho \ell V_2^2 = (p_s - p_o) \ell + \rho (\ell - a) V_S^2 + \rho a V_J^2$$

$$p_o = p_S + \frac{\rho}{2} V_S^2$$

$$(\ell - a) V_S + a V_J = \ell V_2$$

Then it is possible to find the thrust

$$T_2 = \rho \ell V_2^2$$

for a jet engine using the same power

$$P_2 = \frac{\rho}{2} a [V_J^3 + (p_S - p_o) V_J]$$

as the free air jet engine (P_1).

For a two-dimensional ejector using the jet flap diffuser one gets the following fundamental equilibrium equations (Figure 8)

$$\rho D V_3^2 + \rho s V_e^2 (1 - \cos\alpha) = (p_s - p_o)\ell + \rho(\ell - a) V_S^2 + \rho a V_J^2$$

$$p_o = p_S + \frac{\rho}{2} V_S^2$$

$$(\ell - a) V_S + a V_J = D V_3$$

The assumption that at the exit of the mixing chamber the fluid presents a uniform velocity profile introduces the following equations:

$$\rho D\, V_3^2 + \rho s V_e^2 (1-\cos\alpha) = (p_i + \rho V_i^2)\ell$$

$$p_i + \frac{\rho}{2} V_i^2 = p_o + \frac{\rho}{2} V_3^2$$

$$DV_3 = \ell V_i$$

Then defining the following parameters:

$$C_J = \frac{\rho s V_e^2}{\rho a V_J^2} \qquad \text{External Jet Momentum Coefficient}$$

$$\sigma = D/\ell \qquad \text{Diffusion Coefficient}$$

$$A = a/\ell \qquad \text{Ejector Parameter}$$

$$\lambda = \frac{V_2}{V_J} \qquad \text{Velocity Ratio}$$

one gets the two following equations

$$(1-2A)\lambda^2 + 2A = \frac{1+\sigma^2}{\sigma^2}\,[A + (1-A)\lambda]^2 \qquad (1)$$

$$\left(\frac{1-\sigma}{\sigma}\right)^2 [A+(1-A)\lambda]^2 = 2A\, C_J(1-\cos\alpha) \qquad (2)$$

This system was solved numerically on a digital computer. Given A, α, λ, from equation (1) the diffusion coefficient is computed:

$$\sigma = \sqrt{\frac{1}{(1-2A)\lambda^2+2A-[A+(1-A)\lambda]^2}}$$

from equation (2) the external jet momentum coefficient is determined.

$$C_J = \left(\frac{1-\sigma}{\sigma}\right)^2 \frac{[A+(1-A)\,\lambda]^2}{2A(1-\cos\alpha)}$$

Then it is possible to compute the thrust of the ejector-jet flap diffuser system

$$T_3 = \rho D V_3^2 + \rho s V_e^2$$

for the same total power used

$$P_3 = \frac{\rho}{2} a[V_J^3 + (p_S - p_o)V_J] + \frac{\rho}{2} s V_e^3$$

by the free air jet engine.

The comparison of the thrust may also be made for a constant speed at the exit of the jet engine. For an unlimited jet power supply one can get as much thrust as desired. The interaction of the system made by an ejector and a jet flap diffuser has a favorable effect as shown in Figure 9.

For fixed total power, this system gives significant thrust augmentation (one can get 2.8 times the thrust of the jet engine). However, it is noted that this occurs for small values of C_J where there exists a maximum in the curve of A versus C_J (Figures 10 and 11) as found previously in paragraph II-1.

These calculations apply also to the axisymmetric case. The nondimensional results and equations will be the same if one takes the following parameters:

$C_J = \dfrac{2\pi\rho s \ell V_e^2}{\pi a^2 V_J^2}$ for the external jet momentum coefficient

$\sigma = D^2/\ell^2$ for the diffusion coefficient

$A = a^2/\ell^2$ for the ejector parameter

Then, as previously shown in Part II. 1, for the same performance, the width of the external jet must be half the one used in the plane case.

Another way to derive these results is presented in Reference 5 That method has the advantage of giving the results in closed form, but for the programming on a digital computer the one described here is easier.

Consideration is now given to the case where the jet flap is fed by bleeding the jet engine in the compressor stages. From Figures 8 and 12 one finds that for a planar ejector-jet flap diffuser system

$$T_J = a(p_S + \rho V_J^2)$$

$$T_e = \rho s V_e^2$$

and for the jet engine alone

$$T = \rho a V_J^{*2}$$

From the previous system of 6 equations one can get:

$$\frac{T_e}{T}(1-\cos\alpha) = \frac{T_J}{T} \quad 1 + \frac{(1-A)\frac{\lambda^2}{2} - \frac{1}{\sigma}[A+(1-A)\lambda]^2}{A(1-\frac{\lambda^2}{2})} \qquad (3)$$

The solution of equations (1) and (3) was programmed on a digital computer to compute the amplification of thrust due to the use of the ejector-jet flap diffuser system which is

$$\dot{I} = \frac{\rho(DV_3^2 + s\,V_e^2)}{T} = \frac{T_e}{T}\cos\alpha + \frac{T_J}{T}\left(1 + \frac{\lambda^2(1-A)}{A(2-\lambda^2)}\right)$$

Figure 12 shows that substantial increases in thrust may be obtained by the use of a jet flap diffuser. Also from the range of best efficiency of the bleeding characteristic, it is seen that a bleeding coefficient $T_2/T = 6\%$ gives the best results, for the specific engine performance used in the example.

III. ANALYSIS OF THE FLOW

The previous analyses are essentially global, and details of the slope of the jet surface, length, pressure and velocity profiles cannot be obtained. So, in this part, some aspects of the flow field will be theoretically presented. This physical problem is very complex, so the solution of the flow field will be done only under the simplifying assumptions of an incompressible, inviscid flow. First a solution is developed assuming a uniform velocity profile in each section of the flow. Then a linearized perturbation theory in two-dimensional flow is presented. Finally the nonlinear planar problem is formulated although no solution is attempted.

1. Physical Problem: Qualitative Analysis of the Flow Field

Consider first the real flow field. It is clear that it is complicated by having an unknown boundary: the jet sheet. In addition viscous effects introduce problems of turbulent entrainment of the surrounding air, and of turbulent mixing between the inner flow and the external jet. These phenomena present energy losses such that the performance which has been predicted in Part II will not be so good. A theoretical approach of these phenomena seems very difficult as it needs the solution of the unsteady Navier-Stokes equations across a curved unknown boundary. Tests to measure the velocity components and the Reynolds stresses across the flow would give a first understanding of the viscous problem, to provide a basis for a theoretical approach with suitable simplifying assumptions. No experimental studies have yet been made. For the jet flap aerofoils, Spence (Ref. 6) finds excellent agreement between linearized

potential theory and experiment. So we assume that viscous phenomena do not significantly affect the jet flap diffuser performance.

Thus in the following the flow is assumed to be both incompressible and inviscid. Figure 13 shows the way the problem is posed, considering only for the planar case the upper part of the flow (the lower one is obtained by symmetry with respect to the plane DE), or for the axisymmetric one the flow in a section plane.

Consider first the planar problem and assume as in Part II that the momentum $\vec{I}_e$ in the external jet, BC, is constant. From the Euler equations, the components of the speed u(x, y), v(x, y) are related to the static pressure p(x, y) by

$$u \frac{\partial u}{\partial x} + v \frac{\partial u}{\partial y} = - \frac{1}{\rho} \frac{\partial p}{\partial x}$$

$$u \frac{\partial v}{\partial x} + v \frac{\partial v}{\partial y} = - \frac{1}{\rho} \frac{\partial p}{\partial y}$$

The internal flow is initially at subatmospheric pressure and expands or diffuses to ambient pressure. The curvature of the jet sheet induces a variation of pressure across it. At each point of the boundary BC, these pressure forces are in equilibrium with the variation of momentum of the internal flow. The equilibrium equations of a slice of fluid [x, x+dx] in the diffusing region of the flow are from an integral method

$$\frac{d}{dx} \int_o^{h(x)} (p+\rho u^2) dy = - \frac{d}{dx} \text{ Ie } \cos\theta(x) \quad (4) \text{ along } \vec{ox}$$

$$p_{y=o} + \frac{d}{dx} \int_o^{h(x)} \rho uv dy = - \frac{d}{dx} \text{ Ie } \sin\theta(x) \quad (5) \text{ along } \vec{oy}$$

The boundary conditions are:

Along the jet sheet ($x \geq 0$): $\dfrac{v(x, h(x))}{u(x, h(x))} = \dfrac{dh(x)}{dx} = \tan\theta(x)$

Along the plane of symmetry DE: $v(x, o) = 0$

From equation (3) one gets, using the first Euler equation:

$$h'(x)\,(p+\rho u^2)_{y=h(x)} + \rho \int_o^{h(x)} \left(\frac{u\partial u}{\partial x} - \frac{v\partial u}{\partial y}\right) dy = -\frac{d}{dx} I_e \cos\theta(x)$$

which becomes by use of the continuity equation

$$h'(x)(p + \rho u^2)_{y=h(x)} - \rho\,[uv]_o^{h(x)} = -\frac{d}{dx}\, I_e \cos\theta(x)$$

or as $p + \frac{\rho}{2}(u^2+v^2) = H_o$

$$h'(x)H_o - \frac{\rho}{2} u^2(h)h'(x)[1+h'^2] = -\frac{d}{dx} I_e \cos\theta(x) = \frac{I_e h'h''}{(1+h'^2)^{3/2}}$$

From equation (4)

$$p_{y=o} + \rho h'(x)\,[uv]_{h(x)} + \rho \int_o^{h(x)} \frac{\partial}{\partial x}(uv)dy = -\frac{d}{dx} I_e \sin\theta(x)$$

one gets by use of continuity and second Euler equations

$$p_{y=o} + \rho\, h'(x)\,[uv]_{h(x)} + \rho[u^2-v^2]_o^{h(x)} = -\frac{d}{dx} I_e \sin\theta(x)$$

which becomes, using the boundary condition $v(x, h(x)) = h'(x)u(x, h(x))$

$$p_{y=o} + \rho\,[u^2(h) - u^2(o)] = -\frac{d}{dx} I_e \sin\theta(x) = \frac{-I_e h''}{(1+h'^2)^{3/2}}$$

Then to get the shape of the jet sheet BC one has to solve the following system of differential equations:

$$h'(x)H_o - \frac{\rho}{2} h'(x)\, u^2(h)\,[1+h'^2] = \frac{I_e h'h''}{[1+h'^2]^{3/2}}$$

$$H_o + \rho \left[u^2(h) - \frac{3}{2} u^2(o)\right] = - \frac{I_e h''}{[1+h'^2]^{3/2}}$$

but one notes immediately that the solution of a system of two equations relating three unknown functions u(h), u(o), h(x) is impossible. Then the problem can only be solved with the knowledge of one of these functions.

Combining these two relations one gets

$$2H_o + \frac{\rho}{2} \left[(1-h'^2)u^2(h) - 3u^2(o)\right] = 0$$

or if $H_o = \frac{\rho}{2} V_o^2$

$$\frac{u(o)}{V_o} = \sqrt{\frac{\left|2\left(\frac{V_o}{u(h)}\right)^2 + (1-h'^2)\right|}{3\left(\frac{V_o}{u(h)}\right)^2}}$$

one notes that if $\frac{V_o}{u(o)} = \frac{V_o}{u(h)} = 1, h' = 0$ which corresponds to the infinite downstream part of the flow. Also, if u(o) = u(h),

$$\frac{u(h)}{V_o} = \frac{u(o)}{V_o} = \sqrt{\frac{2}{2+h'^2}}$$

Thus the assumption that the horizontal component of the velocity is the same at the boundary of the jet sheet and on the center line is equivalent to the one that the slope of the jet sheet is very small ($h'^2 \ll 1$). In such a case this component will not be very different from the downstream velocity V_o. This assumption is considered in the following paragraph where in each section the velocity profile is assumed to be uniform.

2. One-Dimensional Planar and Axisymmetric Analysis

In this paragraph one considers the one-dimensional flow in a jet flap diffuser. This means that the velocity profile in each section is assumed uniform, so that the vertical component of the velocity is small and neglected.

In the planar case the longitudinal equilibrium equation of a slice of fluid $[x, x+dx]$ in the diffusing region is:

$$\frac{d}{dx}\left[h(x)\,(p(x) + \rho u^2(x))\right] = -I_e \frac{d\cos\theta(x)}{dx}$$

Its integration using the boundary condition that if $x \to \infty$ $\theta = 0$ $u = V_o$ $p = p_o$ = o $h = D$ and the Bernoulli relation: $p(x) + \frac{\rho}{2} u^2(x) = \frac{\rho}{2} V_o^2$ gives:

$$h(x)\,(p(x) + \rho\, u^2(x)) - \rho D\, V_o^2 = I_e\,(1-\cos\theta(x))$$

which can be written in nondimensional form as $C_J = \dfrac{I_e}{\frac{\rho}{2} V_o^2 \ell}$,

$\sigma = D/\ell$, $H(x) = \dfrac{h(x)}{\ell}$, $\dfrac{u(x)}{V_o} = U(x)$, $X = \dfrac{x}{\ell}$, $H(x)U(x) = \sigma$

and $h'(x) = \tan\theta$, $\cos\theta = \dfrac{1}{\sqrt{1 + h'^2}}$

$$H\left(1 + \frac{\sigma^2}{H^2}\right) - 2\sigma = C_J\left(1 - \frac{1}{\sqrt{1-H'^2}}\right)$$

if H is considered as a function of x/ℓ.

Then $$H' = \sqrt{\frac{(H + \frac{\sigma^2}{H} - 2\sigma - C_J)^2 - C_J^2}{(H + \sigma^2/H - 2\sigma - C_J)^2}}$$

and it is possible to integrate the differential equation

$$\frac{H(C_J+2\sigma-H+\frac{\sigma^2}{H})dH}{(\sigma-H)\sqrt{H^2+\sigma^2-2\sigma H-2C_J H}} = dX$$

with the boundary condition H = 1 if X = 0

$$X = \sqrt{2C_J-(\sigma-1)^2} - \sqrt{2C_J H-(\sigma-H)^2} + \sqrt{\frac{C_J\sigma}{2}}\log\left|\left(\frac{\sigma-1}{\sigma-H}\cdot\right.\right.$$

$$\left.\left.\frac{\sqrt{\frac{C_J}{2\sigma}(2C_J H-(\sigma-H)^2)}+\sigma+H}{\sqrt{\frac{C_J}{2\sigma}(2C_J-(\sigma-1)^2)}+\sigma+1}\right)\right|$$

The shape of the jet sheet and the pressure distribution, obtained under such assumptions, are presented on Figure 17 where it is compared with the one obtained from the two-dimensional potential analysis which will be presented in the following part.

Let us now consider the axisymmetric flow under the same assumptions. The longitudinal equilibrium equation of a slice of fluid $[x, x+dx]$ in the diffusing region is:

$$\frac{d}{dx}\pi h^2(x)\,(p(x)+\rho u^2(x)) = -\frac{d}{dx} I_e \cos\theta(x)$$

which, integrated once, becomes:

$$\pi h^2(x)\,(p(x)+\rho\, u^2(x)) - \pi D^2 \rho V_o^2 = I_e\,(1-\cos\theta)$$

as if $x \to \infty$ $h(x) = D$ $p = p_o = 0$ $u = V_o$.

Using the axisymmetric parameters defined previously one can find if

$$\sigma = \frac{D^2}{\ell^2}, \quad H = \frac{h}{\ell}, \quad C_J = \frac{I_e}{\pi \ell^2 \frac{\rho}{2} V_o^2}, \quad U = \frac{u(x)}{V_o},$$

$$X = \frac{x}{\ell}$$

and $$p(x) + \frac{\rho}{2} u^2(x) = \frac{\rho}{2} V_o^2, \quad H^2 U = \sigma, \quad \cos\theta = \frac{1}{\sqrt{1 + h'^2}}$$

$$H^2\left(1 + \frac{\sigma^2}{H^4}\right) - 2\sigma = C_J \left(1 - \frac{1}{\sqrt{1 - H'^2}}\right)$$

Then one has to integrate the following differential equation

$$\frac{dH}{dx} = \frac{\sigma - H^2}{C_J H^2 - (H^2 - \sigma)^2} \sqrt{(\sigma - H^2)^2 - 2C_J H^2}$$

with the boundary value. $H = 1$ if $X = 0$. This integration could be done numerically.

3. Two-Dimensional Potential Analysis

A. Physical Problem

To solve the details of the flow the planar problem was posed as in Figure 13. One considers only the upper part of the flow, the lower one is obtained by symmetry with respect to the plane DE.

The flow of constant velocity V_1 in the infinite upstream section of the canal is expanded downstream to the ambient pressure p_o and a constant speed V_o. At the exit of the canal a thin high velocity jet of constant momentum is blown at an angle α. In this point B, a vertical component of the velocity is created at the upper boundary of the main flow. The jump of pressure across the jet sheet BC decreases as its radius of curvature increases. The static pressure of the main flow finally becomes ambient at downstream infinity.

The jet sheet represents an unknown boundary of the flow: here we have the situation that the shape of the boundary dictates the pressure while the pressure dictates the shape of the boundary, a typical source of an integral equation.

In the following, the external jet is assumed to be thin so the gradient of pressure across it can be written

$$p-p_o = \frac{\rho s V_e^2}{R}$$

where R represents the local radius of curvature.

A standard linearization and normalization gives

$$\bar{u} = \frac{u}{V_1} - 1 \quad (|\bar{u}| \ll 1)$$

$$\bar{v} = \frac{v}{V_1} \ll 1$$

$$\sigma - 1 \sim a\sqrt{C_J/2} << 1$$

If y/ℓ represents the analytic function of x/ℓ for the boundary BC:

The pressure equilibrium across the external jet is:

$$C_p = \frac{p-p_o}{\frac{\rho}{2} V_o^2} = 1-\sigma^2\ ((1+\bar{u})^2 + \bar{v}^2) = \frac{C_J \frac{d^2 y/\ell}{dx/\ell^2}}{(1+\frac{dy/\ell^2}{dx/\ell})^{3/2}}$$

The kinematic condition between the internal flow and the external jet is:

$$\frac{\bar{v}}{1+\bar{u}} = \frac{d\ y/\ell}{d\ x/\ell}$$

Then the linearization gives the boundary condition across BC

$$\bar{u} = -a\sqrt{C_J/2} - \frac{C_J}{2} \frac{d\bar{v}}{d\ x/\ell}$$

The problem then reduces to finding the harmonic functions $\bar{u}$ and $\bar{v}$, in the domain ABCDE, which satisfy the following boundary conditions:

Along AB and DE $\bar{v} = 0$

Along BC $\quad \bar{u} = -a\sqrt{C_J/2} - \frac{C_J}{2} \frac{d\bar{v}}{dx/\ell}$

Along EA $\quad \bar{u} = \bar{v} = 0$

Along DC $\quad \bar{u} = -a\sqrt{C_J/2} \quad \bar{v} = 0$

Two ways of solving the problem are indicated: (Figure 14).

i) Since $\sigma - 1 << 1$ $\bar{v} << 1$ it may be assumed that the line BC is not very different from the straight line BC', so that $\bar{u}$ and $\bar{v}$ may be evaluated along the slit ABC'DE.

ii) To consider the domain ABCDE in the ϕ-ψ plane and to write the boundary conditions in terms of $\overline{\phi} = \frac{\phi}{\ell V_1}$ and $\overline{\psi} = \frac{\psi}{\ell V_1}$. In this case, the condition along BC becomes:

$$\overline{u} = -a\sqrt{C_J/2} - \frac{C_J}{2}\frac{d\overline{v}}{d\overline{\phi}}$$

It is interesting to note that these two ways of considering the physical problem give the same mathematical problem. Thus

$$\overline{u}_i(x/\ell,\ y/\ell) = \overline{u}_{ii}(\overline{\phi},\overline{\psi})$$

$$\overline{v}_i(x/\ell,\ y/\ell) = \overline{v}_{ii}(\overline{\phi},\overline{\psi})$$

if $\quad x/\ell = \overline{\phi} \quad y/\ell = \overline{\psi}$ *

B. Conformal Mapping - Asymptotic Expansions of $\overline{v}$ as $X \to 0$ and $X \to 1$

To find $\overline{u}$ and $\overline{v}$ it is more convenient to map the slit ABCDE into the upper half-plane [Z] (Figure 15) by use of the relationship

$$z/\ell = x/\ell + i\, y/\ell = -\frac{1}{\pi}\log Z + i$$

or $\quad \overline{F} = \overline{\phi} + i\overline{\psi} = -\frac{1}{\pi}\log Z + i$

This results in the existence of two singular points, one at C(X = 0), the other at B (X = 1).

As shown by the global equilibrium equations, the analytic equation $y/\ell\,(x/\ell)$ of the jet sheet BC presents a horizontal asymptote as $x/\ell \to \infty$ (or $\overline{\phi} \to \infty$) so an asymptotic expansion around C is

$$y/\ell = \sigma - \frac{A}{x/\ell} + O\left(\frac{1}{x/\ell}\right)^2 \quad (A > 0)$$

*These symbols are only used here and are defined in the Notation.

then

$$\bar{v} = \frac{d\, y/\ell}{d\, x/\ell} = + \frac{A}{(x/\ell)^2} + O\left(\frac{1}{x/\ell}\right)^3$$

and it gives, in the mapped plane A, as $X \to 0$

$$\bar{v} = \frac{A\pi^2}{(\mathrm{Log}X)^2} \to 0\,, \quad \frac{d\bar{v}}{dX} = - \frac{2A\pi^2}{X(\log X)^3} \to +\infty$$

$$\bar{u} = -a\sqrt{C_J/2} - \frac{AC_J\pi^3}{(\mathrm{Log}X)^3} \to -a\sqrt{C_J/2}\,, \frac{d\bar{u}}{dX} = \frac{3AC_J\pi^3}{X(\mathrm{Log}X)^4} \to +\infty$$

One notes the following results which agree with the global one:

$$\text{as } \bar{v} = \frac{A}{(x/\ell)^2} + O\left(\frac{1}{x/\ell}\right)^3 \quad \text{if } x/\ell \to \infty$$

the integral $\int_o^\infty \bar{v}\, dx/\ell$ which represents the diffusion coefficient σ is convergent

$$\text{as } \frac{d\bar{v}}{dx/\ell} = - \frac{2A}{(x/\ell)^2}\,, \text{ the pressure coefficient}$$

$C_p = C_J \frac{d\bar{v}}{dx/\ell} = - \frac{2AC_J}{(x/\ell)^3}$ then the integrals

$$\int_o^\infty C_p\, dx/\ell \quad \text{and} \quad -\int_o^\infty C_p\, dy/\ell = -\int_o^\infty vC_p\, dx/\ell$$

which represent the components along $\vec{oy}$ and $\vec{ox}$ of the force acted by the inner flow upon the jet sheet are convergent.

In B, $\bar{v} = a$ the function $\bar{u}(X)$ can be found by the Hilbert Transform as $X \to 1$

$$\bar{u}(X) = \lim_{X \to 1} \frac{1}{\pi} \int_o^1 \frac{v(\xi)d\xi}{X - \xi}$$

Let us take b such that if $b \leq \xi \leq 1$ $a-\varepsilon \leq \bar{v}(\xi) \leq a$, as the function $\bar{v}(\xi)$ is continuous on $[0, 1]$

$$\lim_{\substack{\varepsilon \to 0 \\ \xi \to 1}}$$

then $$\bar{u}(X) = \frac{1}{\pi} \int_0^b \frac{\bar{v}(\xi)d\xi}{X-\xi} + \frac{1}{\pi} \int_b^1 \frac{\bar{v}(\xi)d\xi}{X-\xi}$$

As one considers the limit as $X \to 1$ the first integral is non-singular. If I is its value, as $X \to 1$ $\bar{u}(X)$ is bounded by:

$$I + \frac{a-\varepsilon}{\pi} \int_b^1 \frac{d\xi}{X-\xi} \leq \bar{u}(X) \leq I + \frac{a}{\pi} \int_b^1 \frac{d\xi}{X-\xi}$$

or

$$I + \frac{a-\varepsilon}{\pi} \log \left|\frac{X-1}{X-b}\right| \leq \bar{u}(X) \leq I - \frac{a}{\pi} \log \left|\frac{X-1}{X-b}\right|$$

Then taking the limit $X \to 1$ $\varepsilon \to 0$ one notes that $\bar{u}(X)$ is unbounded as $-\frac{a}{\pi} \log |X-1|$. So from the boundary condition

$$\bar{u}(X) = -a\sqrt{C_J/2} + \frac{\pi C_J X}{2} \frac{d\bar{v}}{dX}$$

one obtains by integrating the asymptotic behavior of

$$\frac{d\bar{v}}{dX} = -\frac{2a}{\pi^2 C_J X} \operatorname{Log} |X-1| + \frac{a}{\pi X} \sqrt{\frac{2}{C_J}}$$

$$\bar{v}(X) = a\left(1 - \frac{1}{3C_J}\right) + \frac{a}{\pi\sqrt{C_J/2}} + \frac{a}{\pi^2 C_J/2} \left[X + \frac{X^2}{2^2} + \ldots + \frac{X^2}{n^2} + \ldots\right]$$

One notes on Figure 16 that the infinite behavior of the slope of the function $\bar{v}(X)$ is hardly perceptible. This is also shown by Lissaman in the jet flap problem (Reference 7).

C. Method of Solution: Mathematical Problem

Writing $U = \frac{\overline{u}}{a}$ $V = \frac{\overline{v}}{a}$ it is necessary to evaluate these harmonic functions in the upper half-plane [Z] subject to the following conditions:

Along AB and DE $V = 0$

In E and A $U = 0$

In D $U = -\sqrt{C_J/2}$

Along CB, U and V are related by

$$U = -\sqrt{C_J/2} + \frac{\pi C_J X}{2} \frac{dV}{dX}$$

In the vicinity of B($X \leq 1$)

$$V \sim (1 - \frac{1}{3C_J}) + \frac{1}{\pi\sqrt{C_J/2}} \text{ Log } X + \frac{2}{\pi^2 C_J} \left[X + \frac{X^2}{2^2} + \ldots + \frac{X^2}{n^2} + \ldots \right]$$

In the vicinity of C($X \geq 0$) $V \sim \frac{B}{(\text{Log}X)^2}$. In this form this is a boundary value problem of the Riemann-Hilbert-Poincaré type.

To obtain a numerical solution two domains (0, a) and (b, 1) in which V is defined by its asymptotic expansions are considered. In the domain [a, b] the function V is defined by N straight-line segments (Figures 15, 16) using a method developed by Lissaman (References 7 and 8). The function V therefore depends on N parameters. The value of U, computed by the Hilbert Transform

$$U(X) = \frac{1}{\pi} \int_0^1 \frac{V(\xi)d\xi}{X - \xi}$$

at the midpoint of each straight-line segment is substituted into the

boundary condition expressed at these points. Thus one obtains N equations of the form

$$U\left(a+(2p+1)\frac{b-a}{2N}\right) = \frac{1}{\pi}\int_o^1 \frac{V(\xi)\,d\xi}{a+(2p+1)\frac{b-a}{2N}-\xi}$$

$$= -\sqrt{C_J/2} + \frac{\pi C_J}{2}\left(a+(2p+1)\frac{b-a}{2N}\right)\frac{V_{p+1}-V_p}{\left(\frac{b-a}{N}\right)}$$

with N unknowns being the left extremity of the N straight-line segments which defines $V(\xi)$.

The integral on the left-hand side was split into the following parts:

$$\frac{1}{\pi}\int_o^1 \frac{V(\xi)d\xi}{a+(2p+1)\frac{b-a}{2N}-\xi} = \frac{V_1}{\pi}\int_o^a \left(\frac{\text{Log } a}{\text{Log } \xi}\right)^2 \frac{d\xi}{a+(2p+1)\frac{b-a}{2N}-\xi}$$

$$+\frac{1}{\pi}\sum_{i=1}^{N}\int_{a+(i-1)\frac{b-a}{N}}^{a+i\frac{b-a}{N}}\left[V_i+\frac{V_{i+1}-V_i}{\frac{b-a}{N}}\left(\xi-a-(i-1)\frac{b-a}{N}\right)\right]\frac{d\xi}{a+(2p+1)\frac{b-a}{2N}-\xi}$$

$$+\frac{1}{\pi}\int_o^1\left[\left(1-\frac{1}{3C_J}\right)+\frac{1}{\pi\sqrt{C_J/2}}\text{Log }\xi+\frac{2}{\pi^2 C_J}\left[\xi+\frac{\xi^2}{2^2}+\ldots+\frac{\xi^n}{n^2}+..\right]\right]\frac{d\xi}{a+(2p+1)\frac{b-a}{2N}-\xi}$$

The first integral was computed numerically by a Simpson subroutine. The last one was computed by the same method; a subprogram using expansion of analytically computable integrals was also used. The influence of the values a and b, of the accuracy in the computation of the integrals, and of the different methods used was checked. The only point to note is that "a" must be less than $e^{-3} \sim 0.05$. For this value, the function

$$V(\xi) = V_1\left(\frac{\text{Log } a}{\text{Log } \xi}\right)^2$$

presents an inflection point.

The numerical method used here converges fast; a difference of less than 0.08 in the values of V is found when N varies from 3 to 15. A numerical convergence analysis of this scheme is presented in the appendix.

The shape of the jet sheet was obtained by numerical integration of

$$y/\ell = 1 + \frac{a}{\pi} \int_X^1 \frac{V(\xi)d\xi}{\xi}$$

and the velocity U along the boundary by

$$U(X) = 1 + \frac{1}{\pi} \int_0^1 \frac{V(\xi)d\xi}{X-\xi}$$

In the case where the problem is considered in the ϕ-ψ plane the coordinates along the jet sheet are given by integrating numerically:

$$\begin{cases} d\,x/\ell = -\dfrac{1+\bar{u}}{\pi((1+\bar{u})^2+\bar{v}^2)} \dfrac{dX}{X} \\ d\,y/\ell = -\dfrac{\bar{v}}{\pi((1+\bar{u})^2+\bar{v}^2)} \dfrac{dX}{X} \end{cases}$$

No sensible differences are found in the results given by considering the problem in the physical plane or in the σ-ψ one.

D. Results: Comparison Between One-Dimensional and Planar Theory

The linear two-dimensional solution (Figure 17) shows the characteristics of the flow to exhibit appreciable variation only in a small region near the exit of the duct, the pressures on the upper and lower boundary of the internal flow being the same at more than half a

width of the duct upstream, and at more than one width downstream from the exit plane. The flow diffuses quickly, developing half of its final increase of width in nearly one radius. On the upper boundary, ABC, a significant variation with respect to x in static pressure occurs at the exit of the duct.

The comparison with the uniform velocity profile theory does not show significant differences. For the case $C_J = 5$, $\alpha = 10^o$, presented on Figure 17, the variations of the jet profile are unnoticeable; very small differences appear in the pressure existing on the center line. The most important difference is shown in the pressure along the boundary ABC. From the linearization the pressure is unbounded in B; on the other hand, for the uniform velocity profile theory, there is no variation of pressure in the duct. As a matter of interest, neither of these results is correct near B, since, as is well known, corner flow requires a full non-linear solution for uniform validity.

From this analysis the performance of the jet flap diffuser is found assuming a constant external jet sheet momentum. Details of the external jet shape, pressure and velocity profiles are found assuming both the above and that the internal flow is one-dimensional or a linearized planar flow. It seems probable that the exact solution may lie between these two cases. The effect of the constant jet momentum assumption could be determined by a nonlinear analysis for a jet of finite thickness. This is a very complex problem and only the outline of a possible approach is presented.

4. Non-Linear Two-Dimensional Problem

A. Formulation of the Problem

One considers a jet of total head He issuing at the exit of a two-dimensional channel at an angle α; the channel contains a uniform flow of lower head H_o and discharges into a constant pressure region (Figure 18). Introduce the complex velocity potential

$$\tilde{w}(z) = \tilde{\phi} + i\tilde{\psi}$$

which has been non-dimensionalized with respect to the volumetric flow rate per unit width of the canal DV_o. If the complex space coordinate $z = x + iy$ is non-dimensionalized with respect to $D\,V_o/V_e$ inside the jet and with respect to D in the internal flow, the complex velocity may be written

$$\frac{d\tilde{w}}{d\tilde{z}} = \tilde{u} - i\tilde{v} = \tilde{q}\, e^{-i\theta}$$

where $\tilde{u}$, $\tilde{v}$ and $\tilde{q}$ have been non-dimensionalized with respect to V_o or V_e depending on whether internal flow or jet velocities are being considered.

The flow region in the z plane is mapped into the $\tilde{w}$-plane as shown in Figure 19. The vortex sheet along BE requires that two velocity potentials be used: $\tilde{\phi}_i$, $\tilde{\phi}_e$. Since the locations of the streamlines BE and CD in the physical plane are not known a priori, it is convenient to formulate this problem in the $\tilde{w}$-plane. For this purpose define the logarithm of the complex velocity by

$$\Gamma(\tilde{w}) = \mathrm{Log}(d\tilde{w}/d\tilde{z}) = \Omega(\tilde{\phi},\tilde{\psi}) - i\theta(\tilde{\phi},\tilde{\psi})$$

The real and imaginary parts of $\Gamma(\tilde{w})$ satisfy the Cauchy-Riemann equations and are harmonic functions in each region. Thus

$$\frac{\partial Q}{\partial \tilde{\phi}} = -\frac{\partial \theta}{\partial \tilde{\psi}}$$

and $$\frac{\partial Q}{\partial \tilde{\psi}} = \frac{\partial \theta}{\partial \tilde{\phi}}$$

$$\nabla^2 Q = 0$$

$$\nabla^2 \theta = 0$$

if $$\nabla^2 = \partial^2/\partial\tilde{\psi}^2 + \partial^2/\partial\tilde{\phi}^2$$

In the infinite upstream and downstream section one requires that the flow is undeflected and uniform in each region:

$$\text{for } \tilde{\phi}_i \to \infty \qquad Q_i(\tilde{\phi}_i, \tilde{\psi}_i) \to 0, \ \theta_i(\tilde{\phi}_i, \tilde{\psi}_i) \to 0$$

$$\text{for } 0 \leq \tilde{\psi}_i \leq 1$$

$$\text{for } \tilde{\phi}_e \to \infty \qquad Q_e(\tilde{\phi}_e, \tilde{\psi}_e) \to 0, \ \theta_e(\tilde{\phi}_e, \tilde{\psi}_e) \to 0$$

$$\text{for } 1 \leq \tilde{\psi}_e \leq 1 + \frac{s_\infty V_e}{D V_o}$$

$$\text{for } \tilde{\phi}_i \to -\infty \qquad Q_i(\tilde{\phi}_i, \tilde{\psi}_i) \to \text{Log}\frac{V_1}{V_o}, \ \theta_i(\tilde{\phi}_i, \tilde{\psi}_i) \to 0$$

Along GF and AB the deflection is fixed. Thus $\theta_i(\tilde{\phi}_i, 0) = 0$ and $\theta_i(\tilde{\phi}_i, 1) = 0$ if $-\infty \leq \tilde{\phi}_i \leq 0$. For later use these equations will be expressed in terms of Q_i. Both may be written in the form

$$\vec{t} \cdot \vec{\nabla}\theta = 0$$

where the gradient is with respect to $(\tilde{\phi}_i, \tilde{\psi}_i)$ and $\vec{t}$ is a unit vector tangent to AB or GF. Using the Cauchy-Riemann equations

$$\vec{t} \cdot \vec{\nabla}\theta = \vec{n} \cdot \vec{\nabla}\Omega$$

where $\vec{n}$ is the normal vector associated with $\vec{t}$ one gets:

$$\frac{\partial \Omega_i}{\partial \tilde{\psi}_i} (\tilde{\phi}_i, 0) = 0 \quad \text{along GF}$$

and $$\frac{\partial \Omega_i}{\partial \tilde{\psi}_i} (\tilde{\phi}_i, 1) = 0 \quad \text{if } -\infty \leq \tilde{\phi}_i \leq 0 \quad \text{along AB}$$

Along CD and BE the static pressure must be continuous. The fixed outside pressure along CD requires that the speed just outside the jet is constant, and its value must be V_e. Therefore

$$\Omega_e(\tilde{\phi}_e, 1 + \frac{s_\infty V_e}{D V_o}) = 0 \quad \text{for } C < \tilde{\phi}_e < \infty$$

and along BE

$$p_i(\tilde{\phi}_i, 1-) = p_e(\tilde{\phi}_e, 1+) \text{ for } \tilde{\phi}_i, \tilde{\phi}_e \geq 0$$

where $p(\tilde{\phi}, \tilde{\psi})$ is the static pressure in the fluid and $\tilde{\phi}_i$ and $\tilde{\phi}_e$ correspond to the same physical point in the z plane. From Bernoulli's equations along BE

$$\rho q_i^2(\tilde{\phi}_i, 1-) - \rho\, q_e^2(\tilde{\phi}_e, 1+) = 2(H_o - H_e)$$

which, applied at an infinite distance downstream becomes:

$$(H_o - H_e) / \frac{\rho}{2} V_o^2 = 1 - \frac{V_e^2}{V_o^2}$$

As $Q = \text{Log } \tilde{q}$ one gets:

$$e^{2Q_i(\tilde{\phi}_i, 1-)} - \frac{V_e^2}{V_o^2} e^{2Q_e(\tilde{\phi}_e, 1+)} = 1 - \frac{V_e^2}{V_o^2}$$

Also across BE the curvature $\frac{1}{R} = \frac{\partial\theta}{\partial s} = q \frac{\partial\theta}{\partial\tilde{\phi}}$ where s represents the arc length along the streamline BE must be continuous. Then

$$V_o e^{Q_i(\tilde{\phi}_i, 1-)} \frac{\partial\theta_i}{\partial\tilde{\phi}_i} = V_e e^{Q_e(\tilde{\phi}_e, 1+)} \frac{\partial\theta_e}{\partial\tilde{\phi}_e}$$

Now we consider the exit BC of the external jet; some assumptions have to be made as a boundary condition along this line is required to solve the problem. So one may consider as shown on Figure 18 that BC is a vertical piece of straight line along which the deflection of the velocity is fixed and equal to α. It is sure that such a flow is impossible to set up experimentally, but, as the external jet is thin in comparison with the internal one, one may expect that the phenomena in this region will be globally represented. Then along BC

$$d\tilde{\phi}_e = \tilde{q}_e \sin\alpha \, d\tilde{y}$$

$$d\tilde{\psi}_e = \tilde{q}_e \cos\alpha \, d\tilde{y}$$

or $$\tilde{\psi}_e - 1 = \cot g\alpha \, \tilde{\phi}_e$$

and the line BC is represented in the $\tilde{\phi}$-$\tilde{\psi}$ plane by a piece of straight line of slope $\frac{\pi}{2} - \alpha$ (see the dashed line on Figure 19).

Along BC the deflection is fixed. Thus

$$\theta e(\tilde{\phi}_e, \tilde{\psi}) = \alpha \quad \text{for } \tilde{\psi} - 1 = \cot g\alpha \tilde{\phi}_e$$

Writing this relation in the form $\vec{t} \cdot \vec{\nabla}\theta = 0$ and using the Cauchy-Riemann equations $\vec{t} \cdot \vec{\nabla}\theta = \vec{n} \cdot \vec{\nabla}Q$ one gets as previously shown

$$-\cos\alpha \frac{\partial Q_e}{\partial \tilde{\phi}_e} + \sin\alpha \frac{\partial Q_e}{\partial \tilde{\psi}} = 0 \quad \text{for } \tilde{\psi}_e - 1 = \cot g\alpha \tilde{\phi}_e$$

Then an infinite velocity point must be placed at point B in the $\tilde{w}_i$ plane to insure the turning of the flow through an angle α. This requires

$$\Gamma_i(\tilde{w}_i) \sim -\frac{\alpha}{\pi} \operatorname{Log} \tilde{w}_i \quad \text{as} \quad |\tilde{w}_i| \to 0$$

In the following we give an outline of an approach to the solution of the non-linear problem. It is believed that these boundary conditions are sufficient to determine the two functions $\Gamma_i(\tilde{w}_i)$ and $\Gamma_e(\tilde{w}_e)$. However, the non-linear boundary conditions which must be applied along BE makes an exact treatment intractable. But, in most practical situations, solutions are required when the total head of the jet is much larger than the one of the internal stream. In these cases asymptotic solutions can be found for $\frac{H_e}{H_o} \to \infty$.

B. Approximate Method of Solution for the Non-linear Two-dimensional Problem

In the following one indicates the application of a perturbation method to this problem. Such a method is presented by Ackerberg and Pal for the solution of the injection of a two-dimensional jet into a uniform stream (References 9 and 10).

Four regions of the flow are considered as shown on Figure 20: Region I, where the outer solution in the jet may be derived. There it is expected that $\frac{s_\infty}{Re} << 1$ and that the variations along the jet in the outer region will be much smaller than those across it $\frac{\partial}{\partial\tilde{\phi}_e} << \frac{\partial}{\partial\tilde{\psi}_e}$. This behavior may be taken into account by altering the scale of $\tilde{\phi}_e : \hat{\phi}_e = \frac{H_o}{H_e}\tilde{\phi}_e$, which will remain of O(1) in the outer region. The thin jet approximation results formally by seeking solutions of the form

$$Q_e(\tilde{\phi}_e, \tilde{\psi}_e) \sim \frac{H_o}{H_e}\,\hat{Q}_e(\hat{\phi}_e, \hat{\psi}_e) + O(\frac{H_o}{H_e})$$

$$\theta_e(\tilde{\phi}_e, \tilde{\psi}_e) \sim \hat{\theta}_e(\hat{\phi}_e, \hat{\psi}_e) + O(1)$$

where the symbol $\hat{}$ is used to denote the asymptotic nature of these solutions when $\frac{H_o}{H_e} \to 0$.

Substituting in the Cauchy Riemann relations between Q and θ and in the boundary conditions across the relevant part of CD and BE, it is possible to find the functions $\hat{Q}_e$ and $\hat{\theta}_e$ by equating the coefficient of each power of $\frac{H_o}{H_e}$.

Region II, where the outer solution in the internal stream may be derived. The velocity potential in the outer part of the internal flow which borders the region of the thin jet approximation must be scaled differently from the potential in the jet. As $q = \frac{\partial\phi}{\partial s}$ far downstream along BE where

$$q_e(\tilde{\phi}_e, 1+) \simeq V_e$$

$$q_i(\tilde{\phi}_i, 1-) \simeq V_o$$

one obtains, equating differential arc-length along each side and integrating

$$\tilde{\phi}_i \sim \frac{V_o}{V_e} \tilde{\phi}_e$$

Then the velocity potential and the stream function are scaled in the outer region of the internal flow by:

$$\hat{\phi}_i = \frac{V_e}{V_o} \tilde{\phi}_i$$

and $$\hat{\psi}_i = \frac{V_e}{V_o} \tilde{\psi}_i \quad \text{for} \quad 0 \leq \tilde{\psi}_i \leq 1$$

The outer expansion is assumed to be of the form

$$\tilde{Q}_i (\tilde{\phi}_i, \tilde{\psi}_i) \sim \hat{Q}_i(\hat{\phi}_i, \hat{\psi}_i) + O(1)$$

$$\tilde{\theta}_i (\tilde{\phi}_i, \tilde{\psi}_i) \sim \hat{\theta}_i(\hat{\phi}_i, \hat{\psi}_i) + O(1)$$

where $\hat{Q}_i$ and $\hat{\theta}_i$ satisfy the Cauchy-Riemann equations with respect to the variables $\hat{\phi}_i, \hat{\psi}_i$. Then applying the boundary conditions across BE one can relate the functions $\hat{Q}_i$, $\hat{\theta}_i$, $\hat{Q}_e$, $\hat{\theta}_e$ and one gets along BE distinct relations between $\hat{Q}_e$ and $\hat{\theta}_e$ for the jet and between $\hat{Q}_i$ and $\hat{\theta}_i$ for the internal flow.

Region III, where the inner solution in the jet may be derived. Near the jet opening an inner solution is necessary to satisfy the boundary condition along BC. One expects that $|\tilde{w}_e - i| = O(1)$ in the region. As one takes the limit as $\frac{H_o}{H_e} \to 0$ one expects:

$$\theta_e(\tilde{\phi}_e, \tilde{\psi}_e) \sim a + \frac{H_o}{H_e} \theta_e^*(\tilde{\phi}_e, \tilde{\psi}_e) + O(\frac{H_o}{H_e}) \text{ when } |\tilde{w}_e - i| = O(1)$$

as though $V_e/V_o \to \infty$ so that the jet would maintain constant a and the inner flow diverge at a constant rate, giving:

$$Qe(\tilde{\phi}_e, \tilde{\psi}_e) \sim \frac{H_o}{H_e} Qe^*(\tilde{\phi}_e, \tilde{\psi}_e) + O(\frac{H_o}{H_e})$$

This limit can be also considered as if the internal flow energy approached zero.

The functions Qe* and θe* are related by the Cauchy-Riemann equations and they must satisfy the boundary conditions along BC, CD and BE. This is done by expanding Qe and θe for $\frac{H_o}{H_e} \to 0$ and equating the coefficient of $\frac{H_o}{H_e}$. Finally one requires that the inner solution for $\tilde{\phi}_e \to \infty$ must merge with the outer one for $\hat{\phi}_e \to 0$ to appropriate orders. This is the usual matching procedure for singular perturbation problems (References 11 and 12).

To solve for Q_i^* it will be useful to map the strip BCDE in the potential plane into the upper half of the further auxiliary plane (Z) using the Schwartz-Christoffel transformation. At the same time one considers the s plane ($s = \sigma + i\eta$) (Figure 21) in which the function Q_1^* is easily found from the boundary conditions.

Region IV, where the inner solution in the internal flow may be derived. The motion appears as a corner flow. An expansion which contains the basic corner flow and which merges with $\hat{\Gamma}_i(\hat{w}_i)$ to two terms when $|\hat{w}_i| \to 0$ is assumed to be of the form

$$\tilde{\Gamma}_i(w_i) \sim -\frac{a}{\pi} \mathrm{Log}(\hat{w}_i) + a_\infty + \frac{H_o}{H_e} \Gamma_i^*(w_i^*) + O(\frac{H_o}{H_e})$$

$$\text{for } |w_i^*| = O(1)$$

where a relation between $\hat{w}_i$ and w_i^* has to be found. This is done by equating differential arc length along BE. Then a simple potential problem may be formulated for $\theta_i^*(\phi_i^*, \psi_i^*)$ in the w_i^* plane. The function θ_i^* is harmonic and it has to satisfy the following boundary conditions:

along AG, AB, and GFE the deflection is zero

along BE the deflection must match with the one found for the inner jet solution.

One notes that when $\frac{H_o}{H_e} \to 0$ a solution of the non-linear two-dimensional problem may be found by using different expansions of harmonic functions satisfying the proper boundary conditions in the four regions described previously. But here one more difficulty occurs: it is a fact that the diffusion ratio is unknown and that it is a function of the total head of the jet and the internal flow and to the ratio of the thickness of the jet at its exit to the width of the canal. Thus the value of Q_i along AG is unknown. An iterative procedure could possibly be set up, where for an assumed diffusion ratio the problem is solved, and from the solution the diffusion coefficient is computed so that a new condition is given. This is then iterated to match. Such a solution seems very complicated, and no attempt to set it up has been made.

IV. SUMMARY AND CONCLUSIONS

The jet flap diffuser seems to be a useful device for increasing the thrust of an actuator of given geometry. Theory predicts large performance gains. It may well have some interesting application in cases where it is impossible to employ a solid diffuser, or when the propulsion system is capable of providing extra power.

Applied to an ordinary jet when power is limited substantial thrust augmentation can be achieved only in a certain range of the parameters: momentum coefficient and thickness ratio of the external jet. Good results are obtained by adding a jet flap diffuser to a shrouded propeller; the range of their values agree with the few experimental results found. Its application to a thrust ejector may be shown to enhance the total ejector thrust considerably; very favorable performances result when the jet flap diffuser is fed by bleeding the jet engine in the compressor stages.

These analyses are essentially global and can only predict the total performance of the jet flap diffuser. To get details of the slope of the jet sheet, length, pressure and velocity profiles, the flow field is theoretically studied under the assumption of an incompressible, inviscid fluid.

The problem is very complex by having an unknown boundary: the jet sheet and some assumptions have to be made. First the jet sheet is assumed to be thin and to contain constant momentum. Under the hypothesis of a uniform velocity profile in each section of the internal flow the two-dimensional and axisymmetric solutions are derived.

Also a linearized study is developed and the resulting Riemann-Hilbert-Poincaré type problem is solved numerically. This analysis shows that the flow is almost one-dimensional with two-dimensional variation only in a small region near the exit of the channel. The internal flow diffuses quickly, acquiring half of its final increase of width in nearly one scale length. A significant variation with respect to x in static pressure occurs at the exit of the canal, although the internal pressure variation with respect to y is small. The mathematical process employed herein converges fast.

For the case where the thin jet approximation is not valid, the non-linear two-dimensional problem is formulated. The method to solve it by a variational process is presented when the total head of the jet is very much higher than the one of the internal flow. Its solution requires an iterative process and seems to be very complex.

While these theories probably require modification to account for turbulent entrainment and other real effects, they represent a first step in understanding the operation of the jet flap diffuser, so that its potential may be developed to produce a practical device.

REFERENCES

1. Lazareff, M.: "Hélices Carénées. Synthèse," Technical Note ARA/NT/89/66. Nord-Aviation (France) (1967).

2. Luu Thoai-Sum,"Contribution a la théorie linéarisée des effets de jets minces et de cavitations calcul des écoulements par analogie rhéoelectrique." Thèse présentée à la Faculté des Sciences de l'Université de Paris. Décembre 1960.

3. Spence, D. A.: "The Lift Coefficient of a Thin Jet-flapped Wing," Royal Society of London Proceedings Vol. 238, p. 46 (January 1957).

4. Steffen, F. W. and Jones, J. R.: "Performance of a wind tunnel model of an aerodynamically positioned variable flap ejector at Mach numbers from 0 to 2.0," NASA T.M. X-1639 (1968).

5. Harris, G. L.: "Miscellaneous Topics in Ejector Technology," California Institute of Technology. Pasadena, California (1969).

6. Spence, D. A.: "Some Simple Results for Two-dimensional Jet-Flap Aerofoils," The Aeronautical Quarterly, Vol. IX, p. 395 (November 1958).

7. Lissaman, P. B. S.: "A Linear Solution for the Jet Flap in Ground Effect," Thesis presented at the California Institute of Technology, Pasadena, California (1966).

8. Lissaman, P. B. S.: "A Linear Theory for the Jet Flap in Ground Effect." A.I.A.A. Journal, vol. 6, No. 7, pp. 1356-1362. July 1968.

9. Ackerberg, R. C., "On the Non-linear Theory of Thin Jets a Problem in Singular Perturbation," Polytechnic Institute of

Brooklyn (1965).

10. Pal, A.: "Solution of a Non-linear Boundary Value Problem in Fluid Mechanics using a Variational Method," Polytechnic Institute of Brooklyn (1965).

11. Kaplun, S. and Lagerstrom, P. A.: "Asymptotic expansions of Navier-Stokes solutions for small Reynolds numbers," J. Math. and Mech. 6, pp. 585-593 (1957).

12. Lagerstrom, P. A.: "Note on the preceding two papers," J. Math. and Mech. 6, pp. 605-606 (1957).

APPENDIX

This is concerned with the truncation error of the numerical scheme used to solve the two-dimensional linear problem. For this problem one has to solve the following integro-differential equation:

$$L(V(X)) = \frac{1}{\pi}\int_0^1 \frac{V(\xi)\,d\xi}{X-\xi} + \sqrt{\frac{C_J}{2}} - \frac{\pi C_J}{2}\, X\,\frac{dV}{dX} = 0$$

by using the numerical scheme

$$L_h(V_i(X)) = \frac{1}{\pi}\int_0^1 \frac{V_1\left(\frac{\text{Log}a}{\text{Log}\xi}\right)^2 d\xi}{a+(2p+1)\frac{b-a}{2N} - \xi}$$

$$+ \frac{1}{\pi}\sum_{i=1}^{N}\int_{a+(i-1)\frac{b-a}{N}}^{a+i\frac{b-a}{N}} \frac{\left(V_i + \frac{V_{i+1}-V_1}{\frac{b-a}{N}}\left(\xi-a-(i-1)\frac{b-a}{N}\right)\right)d\xi}{a+(2p+1)\frac{b-a}{2N} - \xi}$$

$$+ \frac{1}{\pi}\int_0^1 \frac{\left(1-\frac{1}{3C_J}\right) + \frac{1}{\pi\sqrt{C_J/2}}\,\text{Log}\,\xi + \frac{2}{\pi^2 C_J}\left(\xi+\frac{\xi^2}{2^2}+\ldots+\frac{\xi^n}{n^2}+\ldots\right)}{a+(2p+1)\frac{b-a}{2N} - \xi} d\xi$$

$$+\sqrt{\frac{C_J}{2}} - \frac{\pi C_J}{2}\left(a+(2p+1)\frac{b-a}{2N}\right)\frac{V_{p+1}-V_p}{\left(\frac{b-a}{N}\right)}$$

Then the truncation error is defined for a sufficiently smooth function f(x) which satisfies the two asymptotic expansions for X = 0 and 1.

$$\tau_p(f(X)) = L_h(f(X_p)) - L(f(X_p))$$

This expression may be divided in four terms

$$\tau_p^1(f(X)) = \frac{1}{\pi}\int_o^a \frac{\left[f_1\left(\frac{\mathrm{Log}a}{\mathrm{Log}\xi}\right)^2 - f(\xi)\right]d\xi}{a+(2p+1)\frac{h}{2} - \xi}$$

$$\tau_p^2(f(X)) = \frac{1}{\pi}\sum_{i=1}^{N}\int_{a+(i-1)h}^{a+ih}\left[f_i + \frac{f_{i+1}-f_i}{h}(\xi-a-(i-1)h) - f(\xi)\right]\frac{d\xi}{a+(2p+1)\frac{h}{2} - \xi}$$

$$\tau_p^3(f(X)) = \frac{1}{\pi}\int_b^1 \frac{\left[\left(1-\frac{1}{3C_J}\right)+\frac{1}{\pi\sqrt{C_J/2}}\mathrm{Log}\xi + \frac{2}{\pi^2 C_J}\left[\xi+\frac{\xi^2}{2^2}+..+\frac{\xi^n}{n^2}+..\right] - f(\xi)\right]d\xi}{a+(2p+1)\frac{h}{2} - \xi}$$

$$\tau_p^4(f(X)) = -\frac{\pi C_J}{2}\left(a+(2p+1)\frac{h}{2}\right)\left(\frac{f_{p+1}-f_p}{h} - f'\left(a+(2p+1)\frac{h}{2}\right)\right)$$

where $h = \frac{b-a}{N}$, f_i is the value of the function $f(\xi)$ at the point $\xi = a+(i-1)h$ and

$$\tau_p(f(X)) = \tau_p^1 + \tau_p^2 + \tau_p^3 + \tau_p^4$$

One gets for $\tau_p^1(f(X))$ as $f(X)$ has the same behavior as $V(X)$ around $X = 0$

$$f(X) = f_1\left(\frac{\mathrm{Log}a}{\mathrm{Log}X}\right)^2 + f_1^*/(\mathrm{Log}X)^3 \quad \text{where } f_1^* \text{ is a bounded constant}$$

$$|\tau_p^1| \leq \frac{1}{\pi(2p+1)\frac{h}{2}}\left|f_1^*\int_o^a \frac{d\xi}{(\mathrm{Log}\xi)^3}\right| \leq \frac{|f_1^*|\,a}{\pi(2p+1)\frac{h}{2}(\mathrm{Log}a)^3}$$

For the second term using Taylor expansions for f_{i+1} and $f(\xi)$:

$$f_{i+1} = f_i + h f_i' + \frac{h^2}{2!} f_i'' + O(h^3)$$

$$f(\xi) = f_i + (\xi-\beta) f_i' + \left(\frac{\xi-\beta}{2!}\right)^2 f_i'' + O(\xi-\beta)^3$$

where $\beta = a+(i-1)h \qquad i = 1, \ldots\ldots, N$

If $\gamma = a+(2p+1)\frac{h}{2} \quad p = 0, \ldots\ldots, N-1$

one gets for the first term approximation of τ_p^2

$$\tau_p^2 (f(X)) \simeq \frac{1}{\pi} \sum_{i=1}^{N} \frac{f_i''}{2!} \int_a^{a+h} \frac{(\xi-\beta)(h-\xi+\beta)}{\gamma-\xi} \, d\xi$$

$$\tau_p^2 (f(X)) \simeq -\frac{1}{\pi} \sum_{i=1}^{N} \frac{f_i''}{2!} \left(\frac{h^2}{2} - h(\gamma-\beta) - (\gamma-\beta)(\gamma-\beta-h)\text{Log}(1+\frac{h}{\beta-\gamma}) \right)$$

On [a, b] $f''(X)$ is bounded, let F'' be the maximum of this second derivative on [a, b]. A bound for the absolute value of τ_p^2 will be

$$\left|\tau_p^2 (f(X))\right| \leq \frac{|F''|}{2\pi} \sum_{i=1}^{N} \left| \frac{h^2}{2} - h(\gamma-\beta) - (\gamma-\beta)(\gamma-\beta-h)\text{Log} \left|1 + \frac{1}{\beta-\gamma}\right| \right|$$

Then the following cases have to be considered:

$\beta-\gamma \geq \frac{h}{2}$ then the logarithm is positive and less than $\frac{h}{\beta-\gamma}$, the result is negative and a bound for the absolute value is $\frac{h^2}{2}$.

$\beta-\gamma = -\frac{h}{2}$ then the logarithm is null and also the absolute value.

$\beta-\gamma \leq -\frac{3h}{2}$ then the logarithm is negative, the result is negative and an expansion for it is:

$$-\frac{h^3}{2!(\gamma-\beta)} + \frac{h^3}{3!(\gamma-\beta)} - \cdots - \frac{h^n}{(n-1)!(\gamma-\beta)^{n-2}} + \frac{h^n}{n!(\gamma-\beta)^{n-2}} - \cdots$$

the term of this series is $-\frac{h^n}{(\gamma-\beta)^{n-2}} \left(\frac{n-1}{n}\right)$ as $\frac{h^{n-2}}{(\gamma-\beta)^{n-2}} \leq \left(\frac{2}{3}\right)^{n-2}$

it is convergent and its limit has the form $-Mh^2$ where M is a positive constant. Then the truncation error term is of order h.

$$\left|\tau_p^2 (f(X))\right| \leq \frac{KF''h}{2\pi} \quad \text{where K is a finite constant.}$$

For τ_p^3 (f(X)) let us look for an error estimate in the asymptotic expansion of f(X) on $[b, 1]$. From the derivation of this expansion (see paragraph III. 3. B) one notes that the error in the expansion is of the order $\frac{2\varepsilon}{\pi^2 C_J} \int_X^1 \frac{d\xi}{\xi} \operatorname{Log} \left|\frac{\xi-1}{\xi-b}\right|$ for $b \leq X \leq 1$ where ε is the variation of V(x) on $[b, 1]$. A bound for this integral is

$$\frac{2\varepsilon}{\pi^2 C_J b} \int_X^1 \operatorname{Log} \left|\frac{\xi-1}{\xi-b}\right| d\xi \leq \frac{2\varepsilon (1-b) \operatorname{Log} \frac{1-b}{2}}{\pi^2 C_J b}$$

Let us now find a maximum for ε

$$\varepsilon = \frac{1}{3C_J} - \frac{1}{\pi\sqrt{\frac{C_J}{2}}} \operatorname{Log} b - \frac{2}{\pi^2 C_J} \left(b + \frac{b^2}{2^2} + \ldots + \frac{b^n}{n^2} + \ldots\right)$$

as $\quad b + \frac{b^2}{2} + \ldots\ldots + \frac{b^n}{n^2} \leq \frac{\pi^2}{6}$

$$\varepsilon \leq - \frac{1}{\pi\sqrt{\frac{C_J}{2}}} \operatorname{Log} b$$

Then

$$\left|\tau_p^3 (f(X))\right| \leq \left| \frac{-(1-b)\operatorname{Log} b \operatorname{Log}\left(\frac{1-b}{2}\right)}{\pi^4 \; b \sqrt{\frac{C_J^3}{8}}} \int_b^1 \frac{d\xi}{a+(2p+1)\frac{h}{2} - \xi} \right|$$

or $\quad \left|\tau_p^3 (f(X))\right| \leq \frac{2(1-b)^2 \operatorname{Log} b \operatorname{Log}\left(\frac{1-b}{2}\right)}{\pi^4 \, b \, h \sqrt{\frac{C_J^3}{8}}}$

If $1-b = \eta << 1$, τ_p^3 is of the order

$$|\tau_p^3 (f(X))| \sim K' \frac{\eta^3 \mathrm{Log}\eta}{h}$$

For $\tau_p^4 (f(X))$ one can expand f_{p+1} and f_p around the point $\gamma = a+(2p+1)\frac{h}{2}$ using the Taylor series:

$$f_{p+1} = f_{p+\frac{1}{2}} + \frac{h}{2} f'_{p+\frac{1}{2}} + (\frac{h}{2})^2 \frac{f''_{p+1/2}}{2!} + (\frac{h}{2})^3 \frac{f'''_{p+1/2}}{3!} + O(h)^4$$

$$f_p = f_{p+\frac{1}{2}} - \frac{h}{2} f'_{p+\frac{1}{2}} + (\frac{h}{2})^2 \frac{f''_{p+1/2}}{2!} - (\frac{h}{2})^3 \frac{f'''_{p+1/2}}{3!} + O(h)^4$$

On $[a, b]$ $f'''(X)$ is bounded; let F''' be the maximum of this third derivative on $[a, b]$. The truncation error τ_p^4 is then bounded by

$$|\tau_p^4 (f(X))| \leq \frac{\pi C_J}{3!} |F'''| \frac{h^2}{8}$$

and the truncation error for this numerical scheme has the order

$$O(\tau_p(f(X))) = \text{max of } O(\frac{a}{h(\mathrm{Log}a)^3}, h, \frac{\eta^3 \mathrm{Log}\eta}{h})$$

Then the numerical scheme $L_h[\cdot]$ is consistent with the integro-differential equation $L[\cdot]$ and has at least an order of accuracy 1.

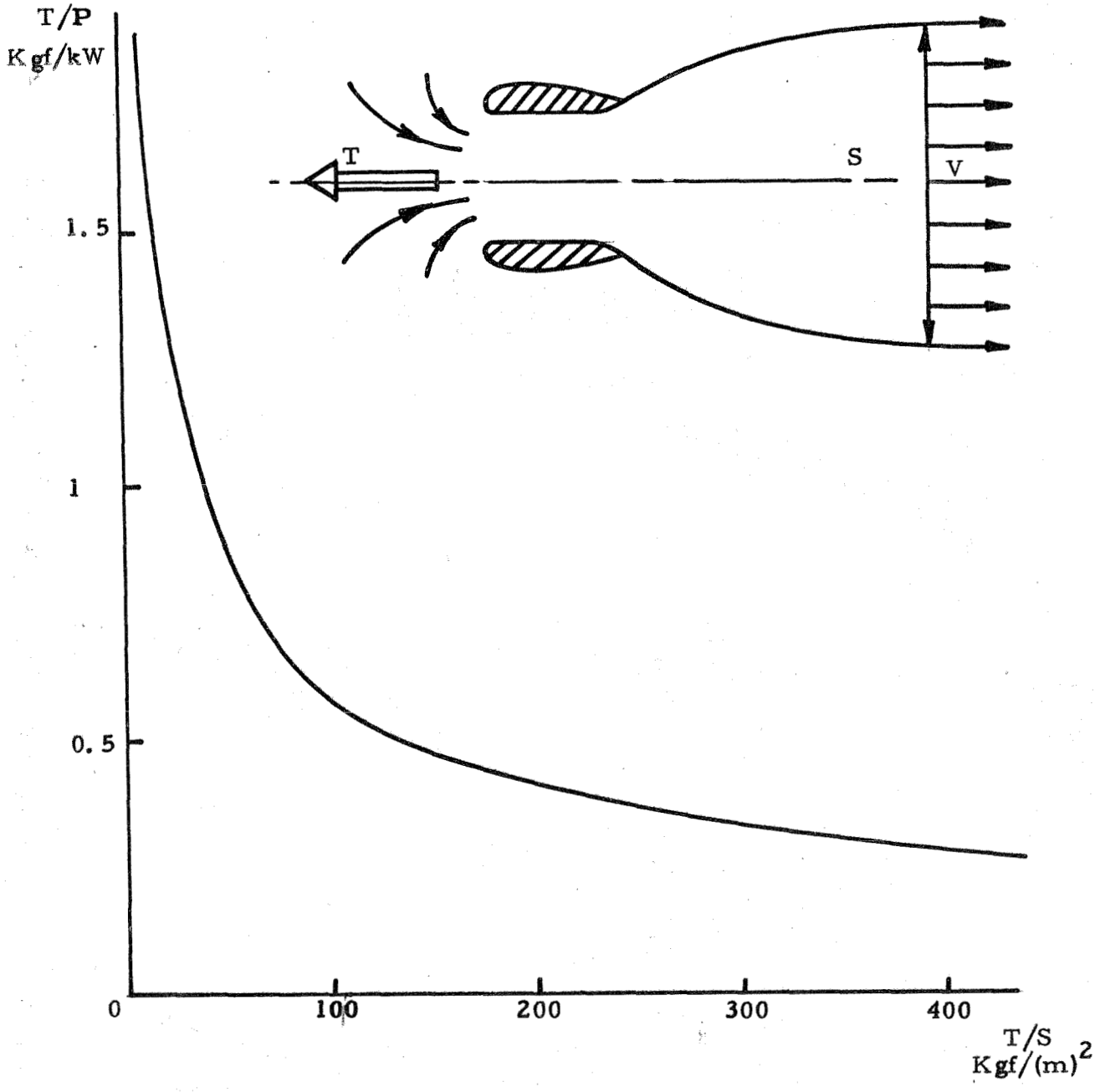

FIGURE 1: THRUST PERFORMANCE OF STATIC PROPULSION SYSTEM

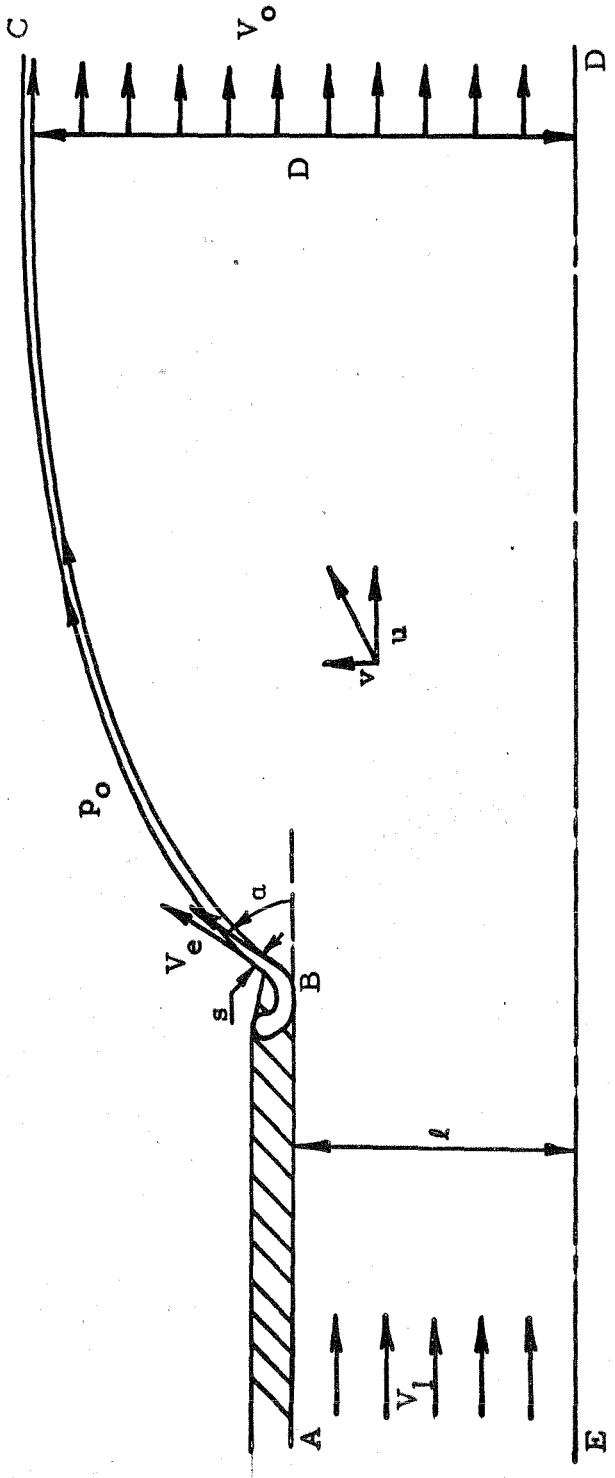

FIGURE 2: GEOMETRY OF JET FLAP DIFFUSER

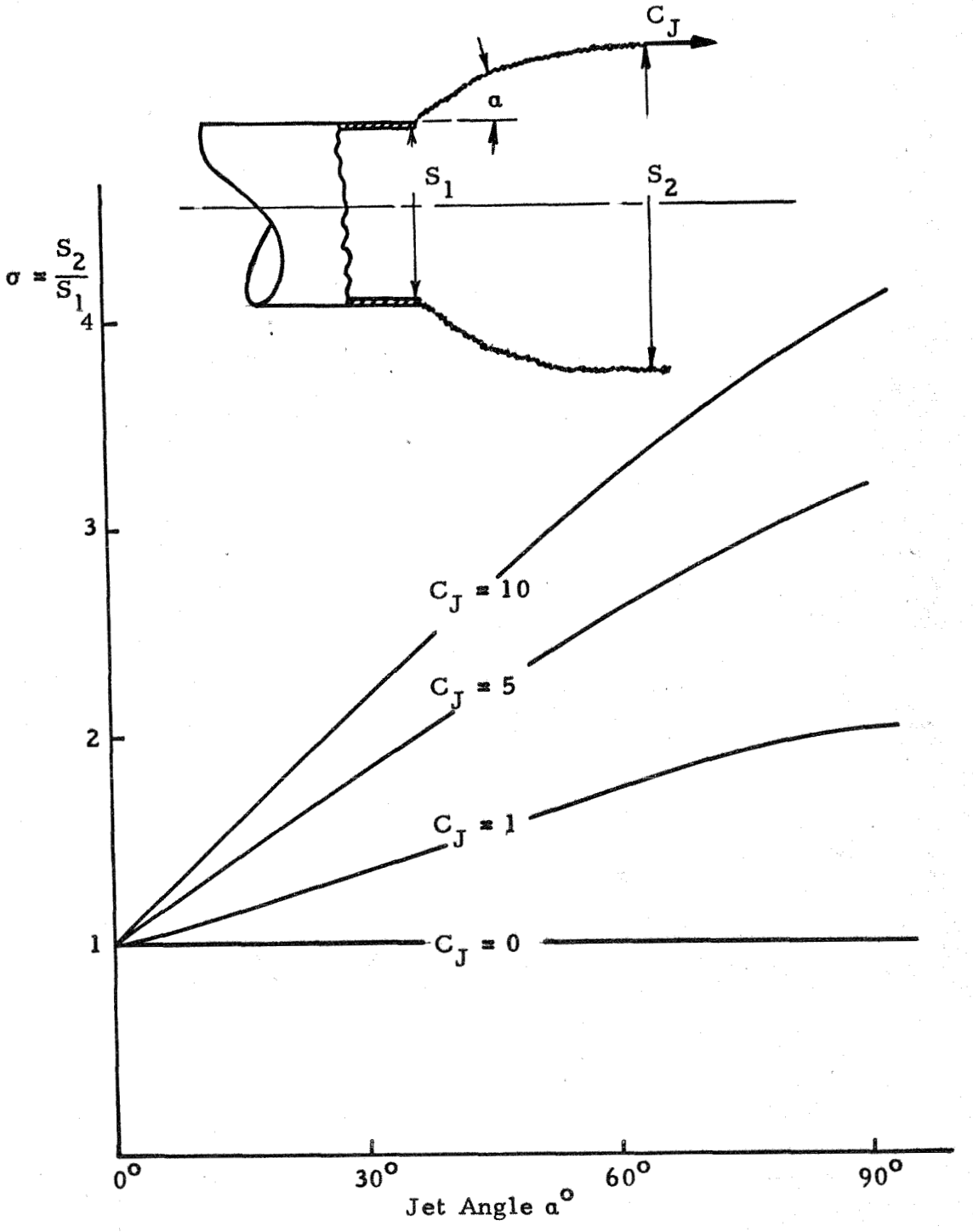

FIGURE 3: DIFFUSION COEFFICIENT
FOR PLANAR AND AXISYMMETRIC FLOW

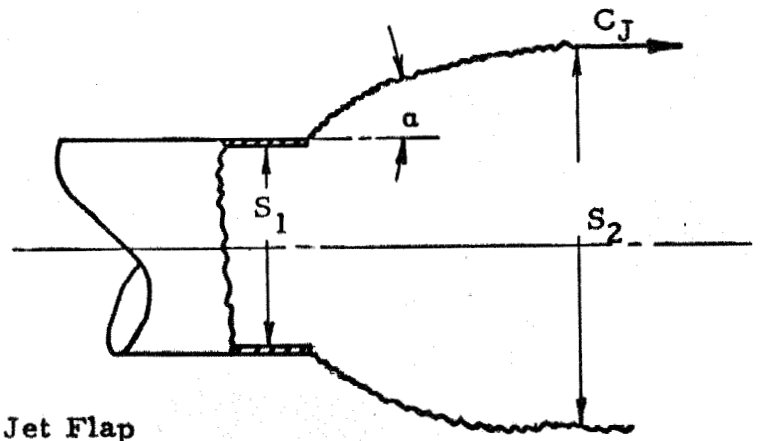

$$[A]_{H_o} = \frac{\text{Thrust with Jet Flap}}{\text{Thrust without}}$$

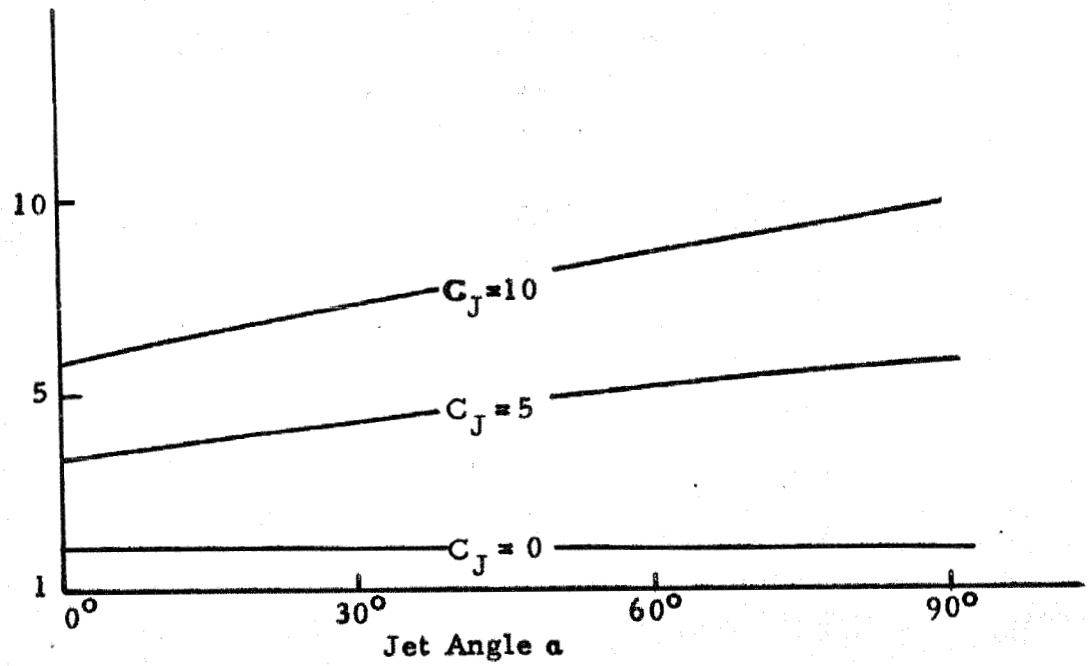

FIGURE 4: AMPLIFICATION FOR GIVEN TOTAL HEAD FLOW

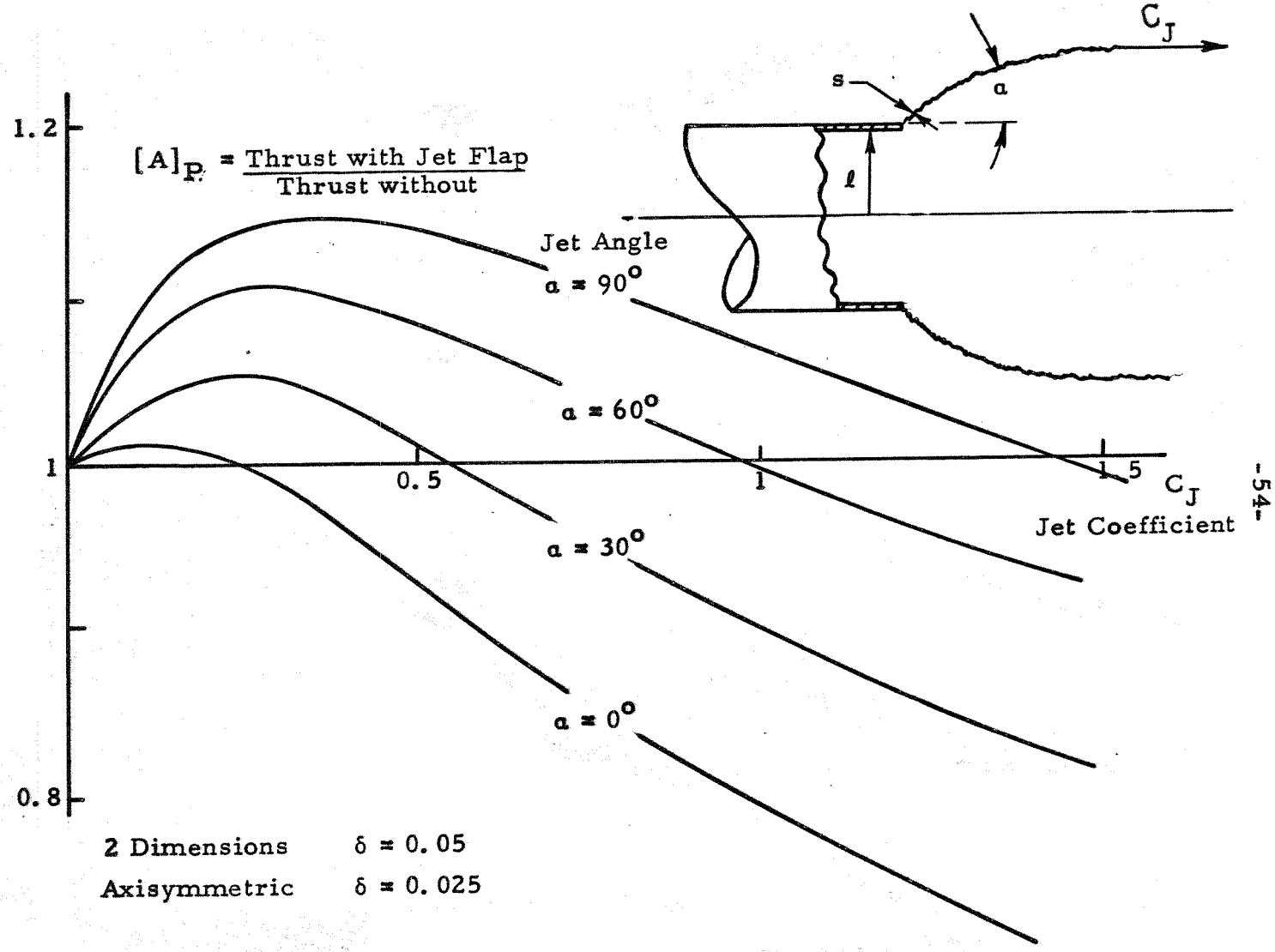

FIGURE 5: AMPLIFICATION FOR GIVEN TOTAL POWER FLOW WITH FIXED JET THICKNESS

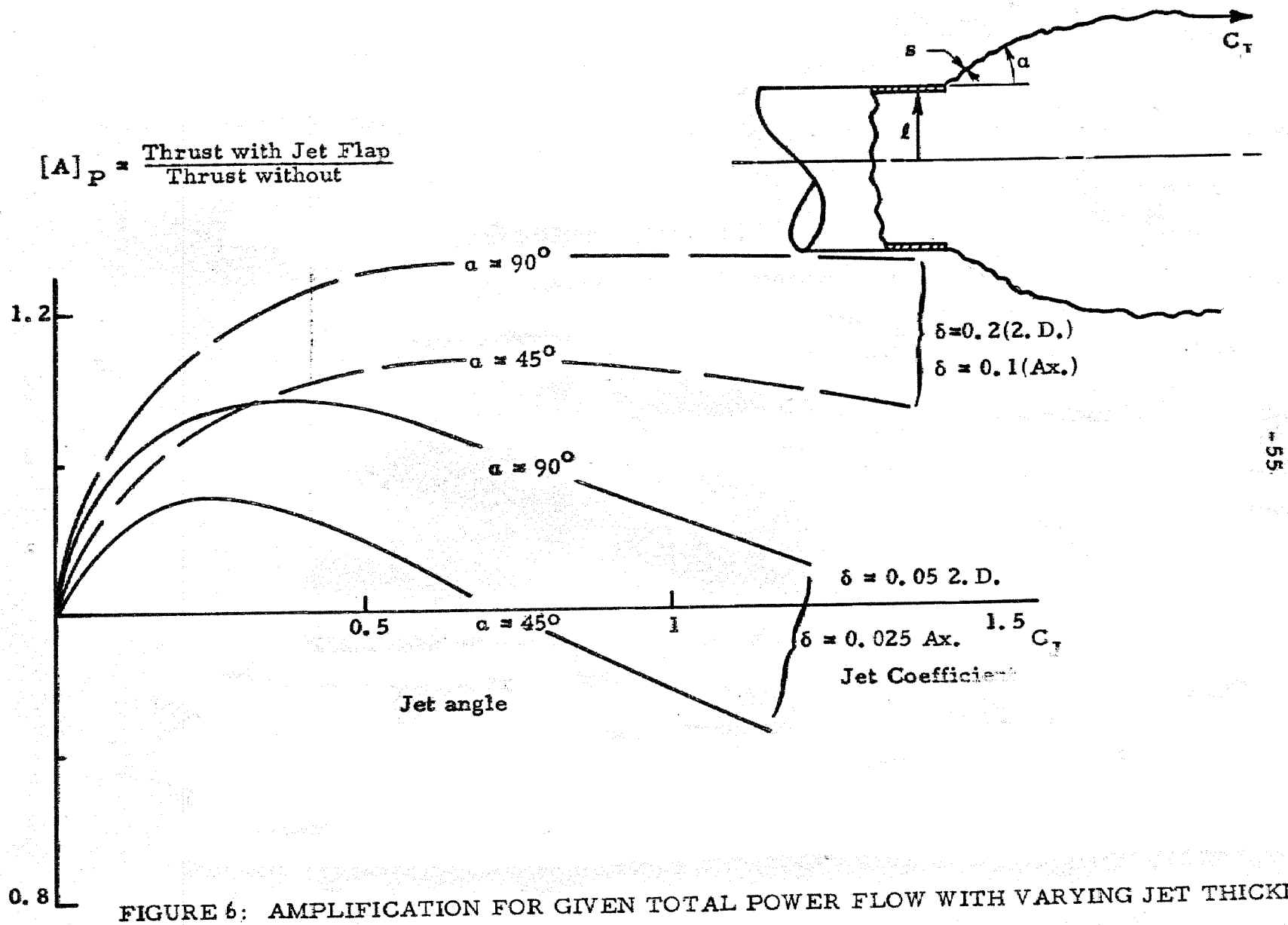

FIGURE 6: AMPLIFICATION FOR GIVEN TOTAL POWER FLOW WITH VARYING JET THICKNESS

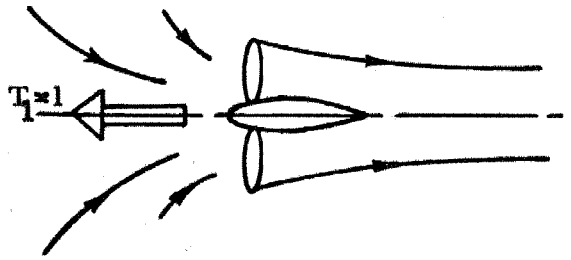

Plain Propeller

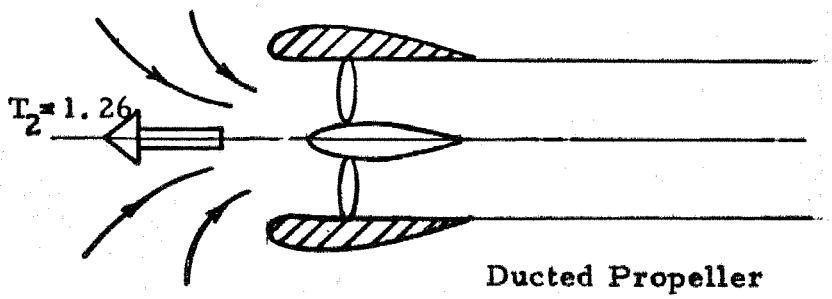

Ducted Propeller

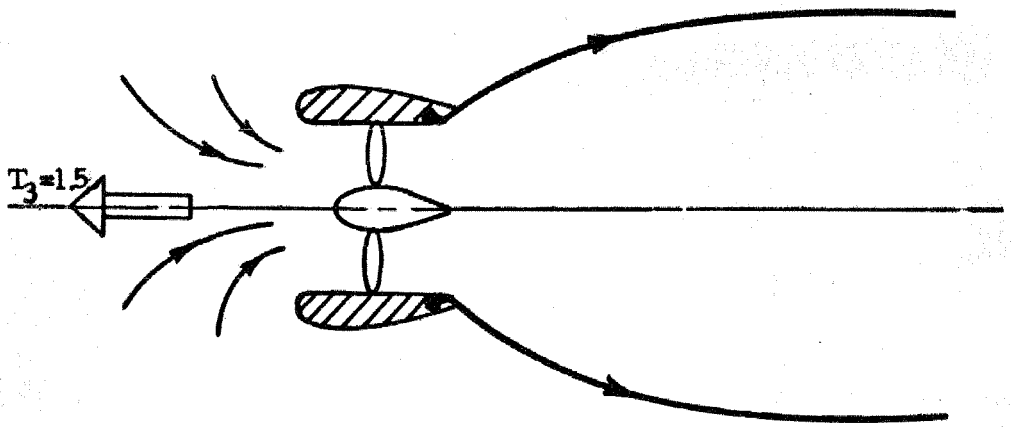

Ducted Propeller with Jet Flap Diffuser

FIGURE 7: COMPARISON OF JET FLAP DIFFUSER WITH CONVENTIONAL ACTUATOR SYSTEM

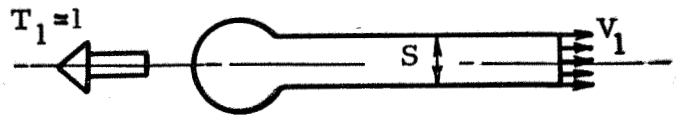

Plain Jet

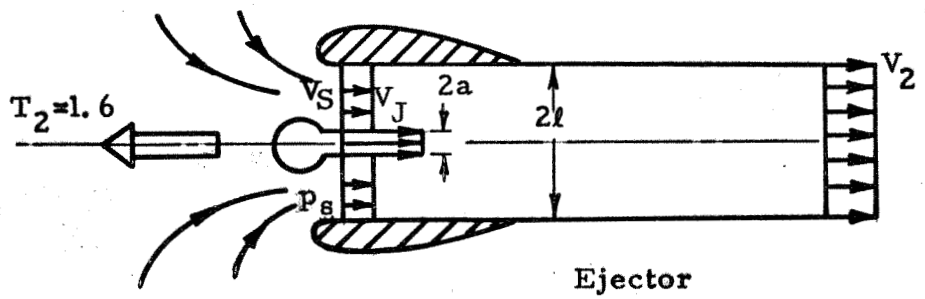

Ejector

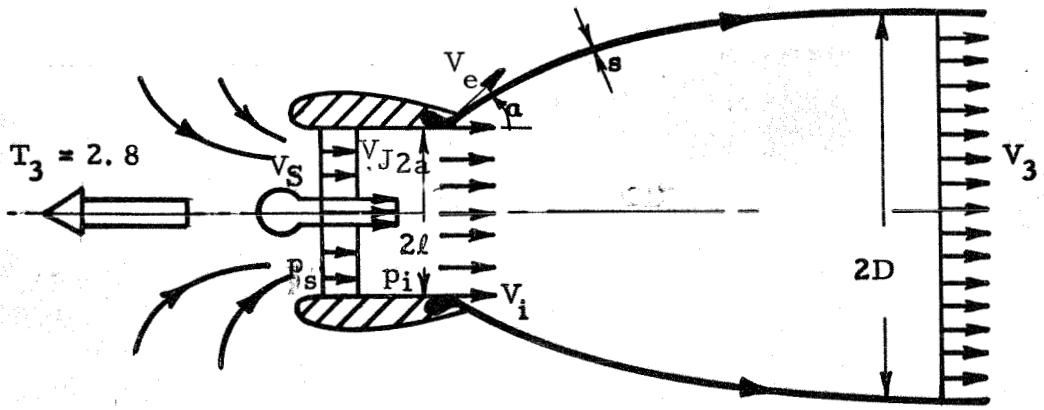

Ejector with Jet Flap Diffuser

FIGURE 8: COMPARISON OF JET FLAP DIFFUSER WITH EJECTOR SYSTEM

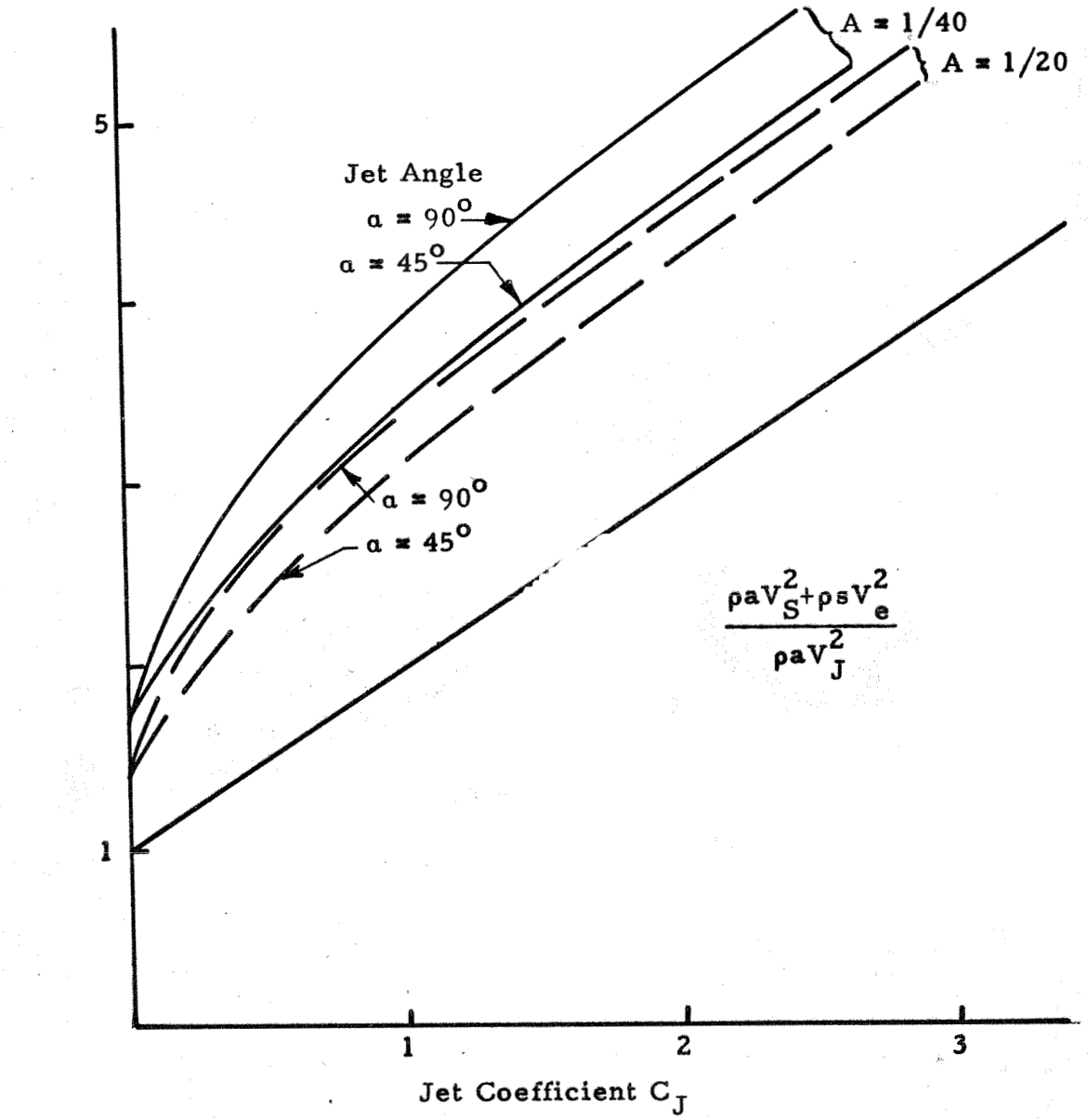

FIGURE 9: COMPARISON OF JET FLAP DIFFUSER/EJECTOR WITH JET ENGINE (FIXED JET SPEED)

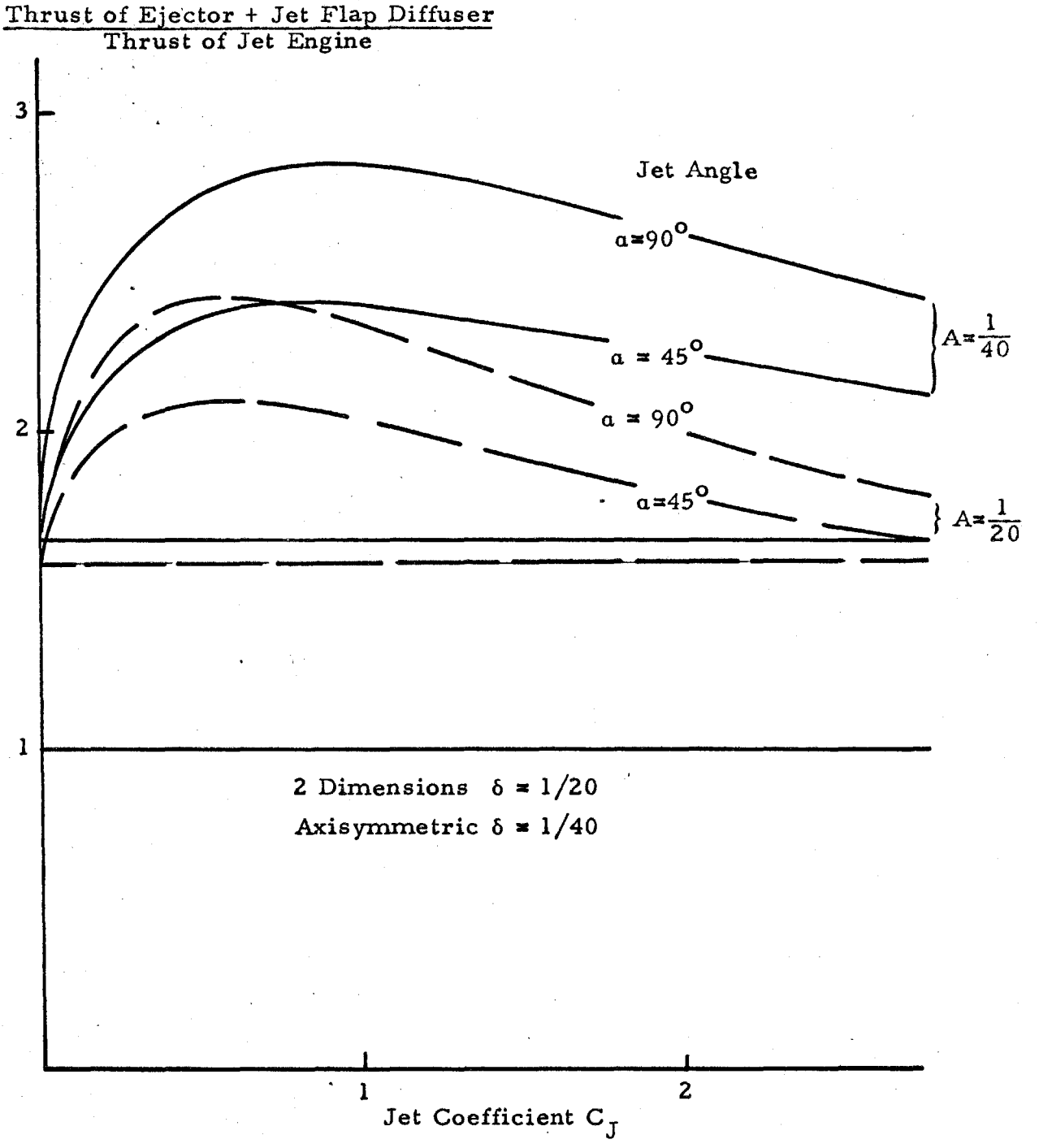

FIGURE 10: COMPARISON OF JET FLAP DIFFUSER/EJECTOR WITH JET ENGINE (FIXED POWER)

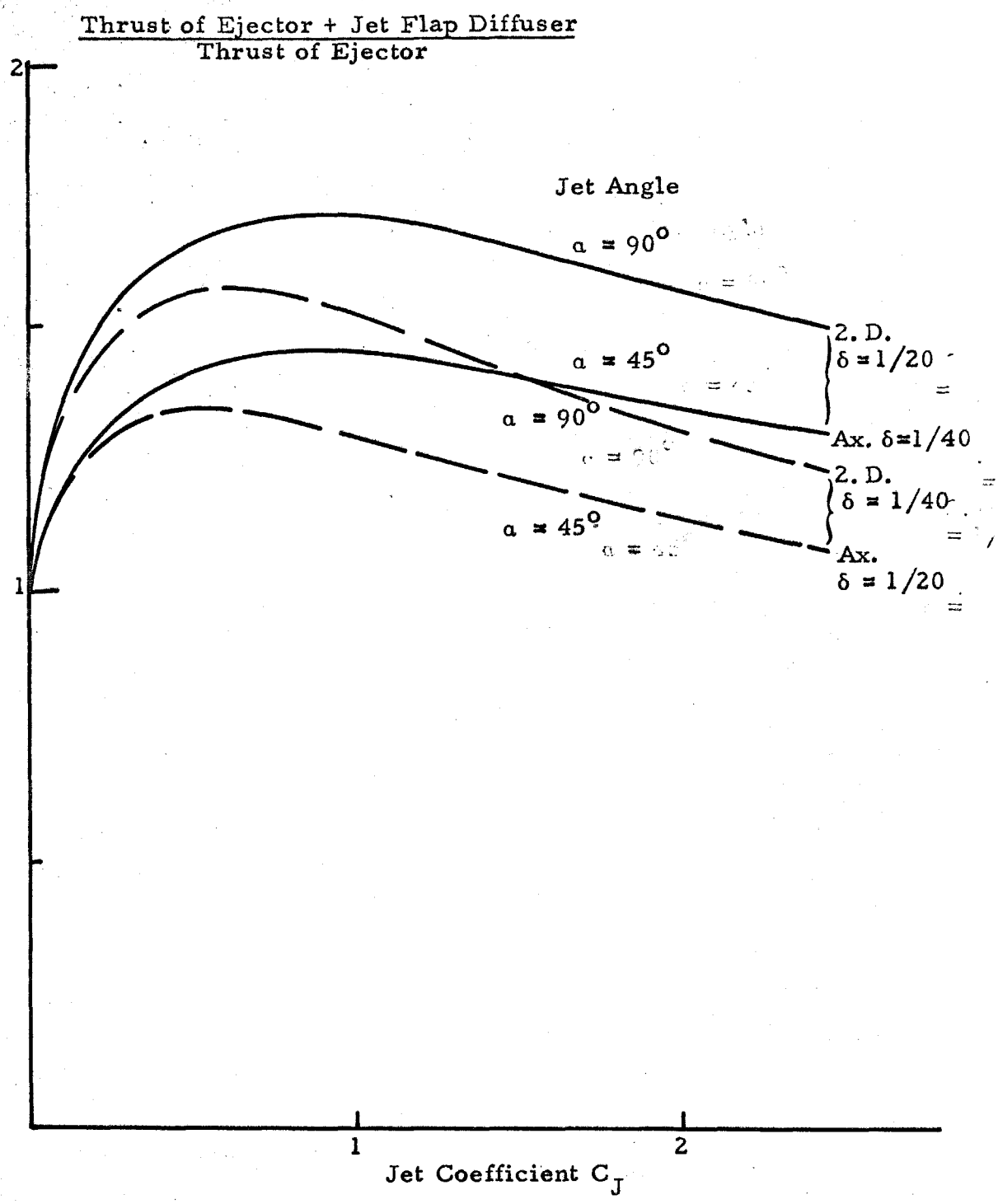

FIGURE 11: COMPARISON OF JET FLAP DIFFUSER/EJECTOR WITH EJECTOR (FIXED POWER)

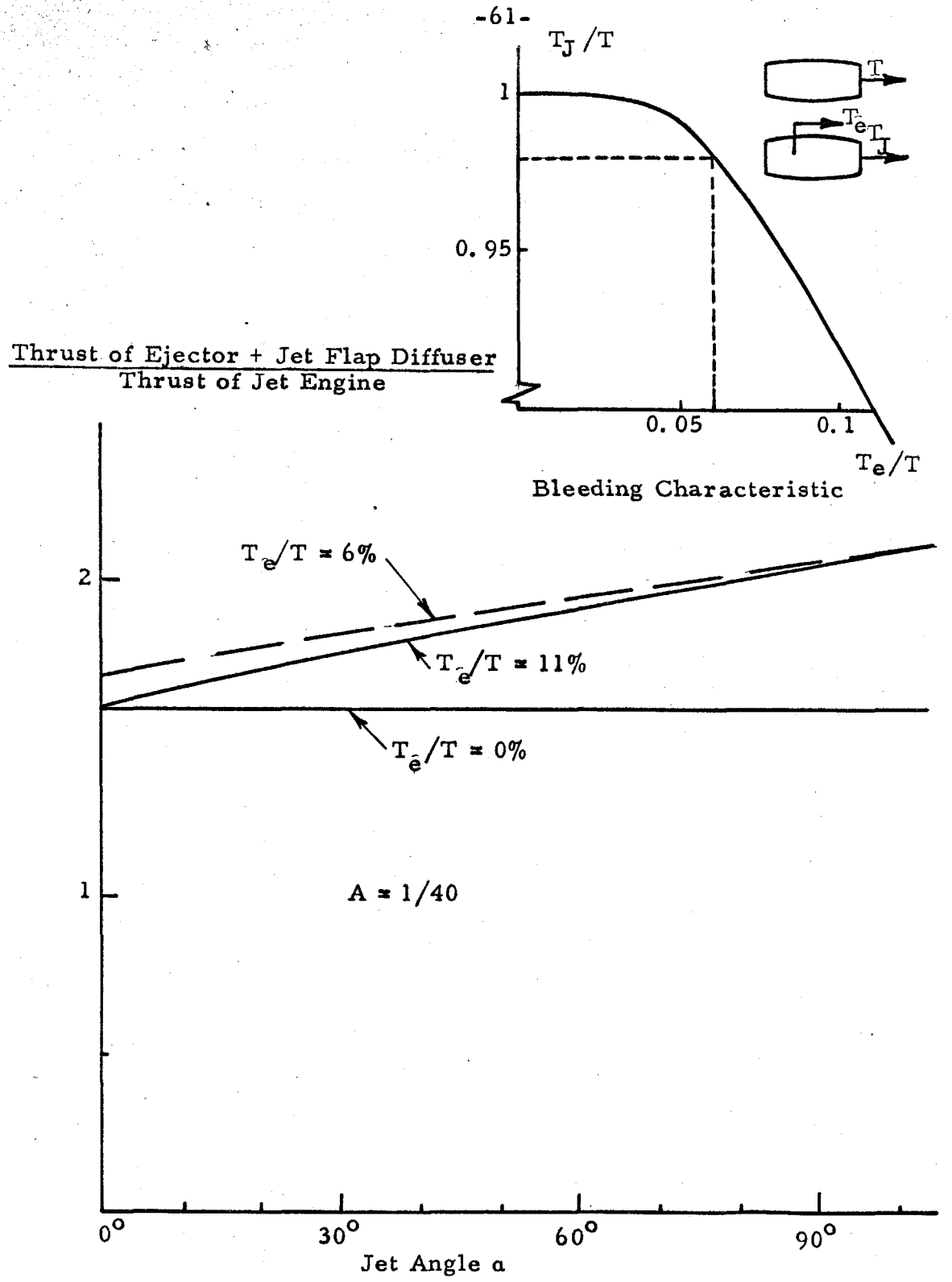

FIGURE 12: PERFORMANCE OF JET FLAP DIFFUSER ON SPECIFIC JET ENGINE

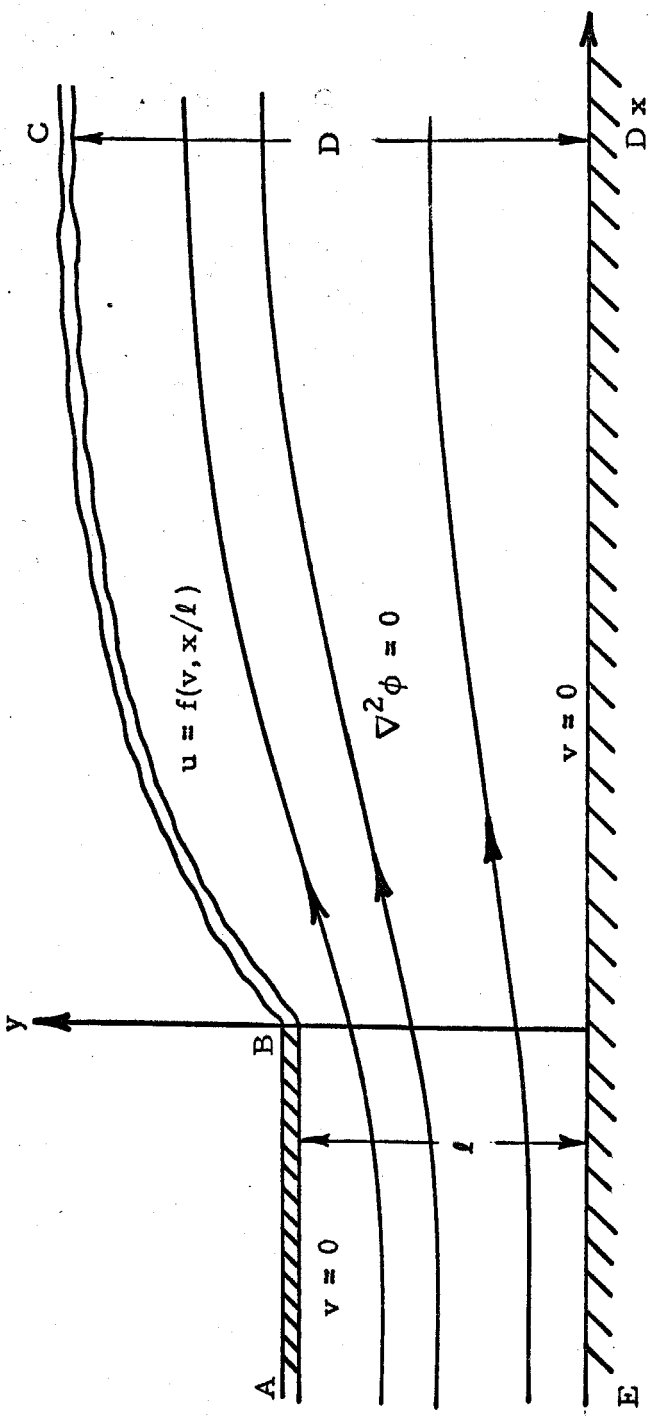

FIGURE 13: GEOMETRY IN THE PHYSICAL PLANE

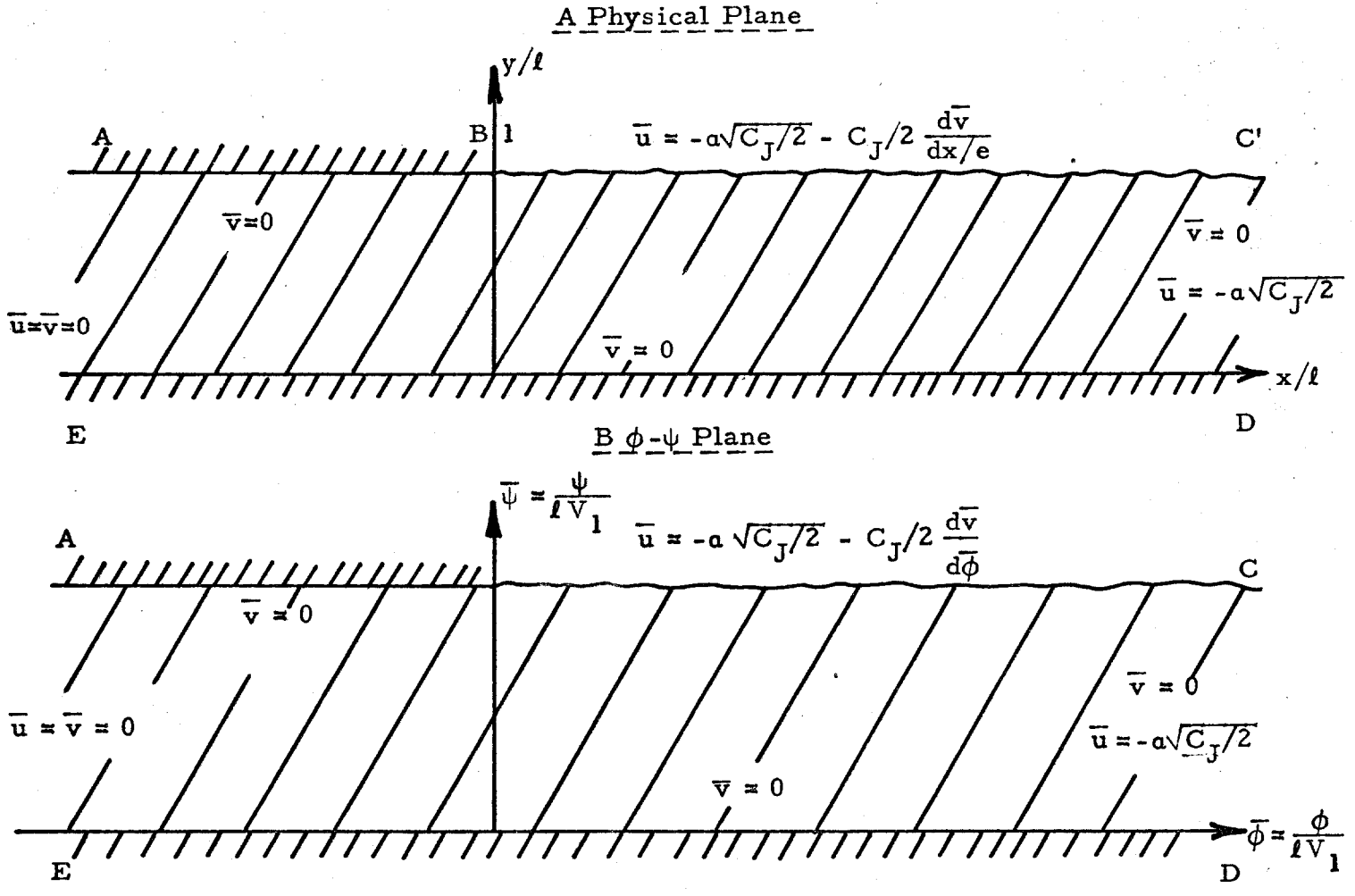

FIGURE 14: LINEARIZED GEOMETRY

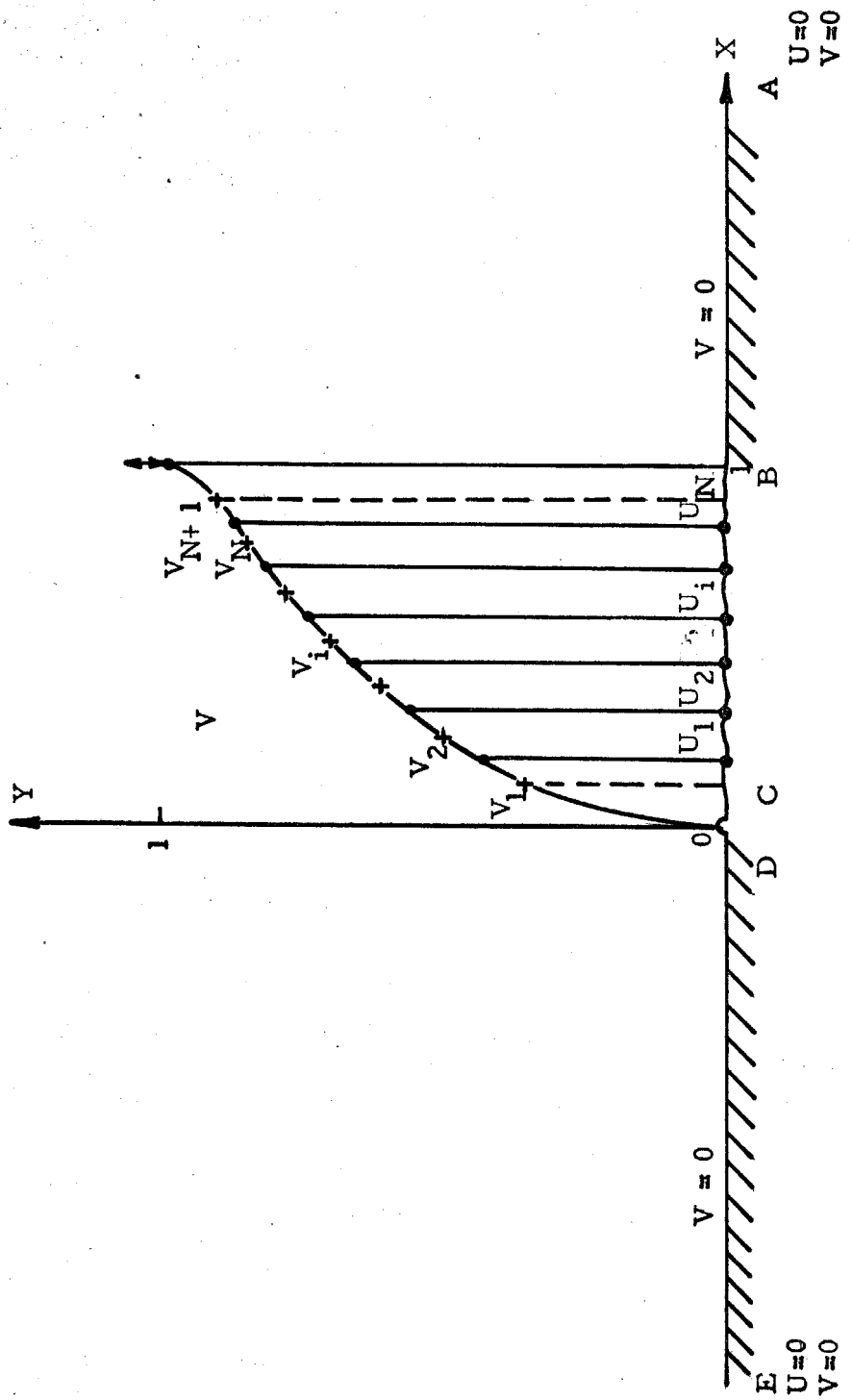

FIGURE 15: V COMPONENT IN AUXILIARY PLANE

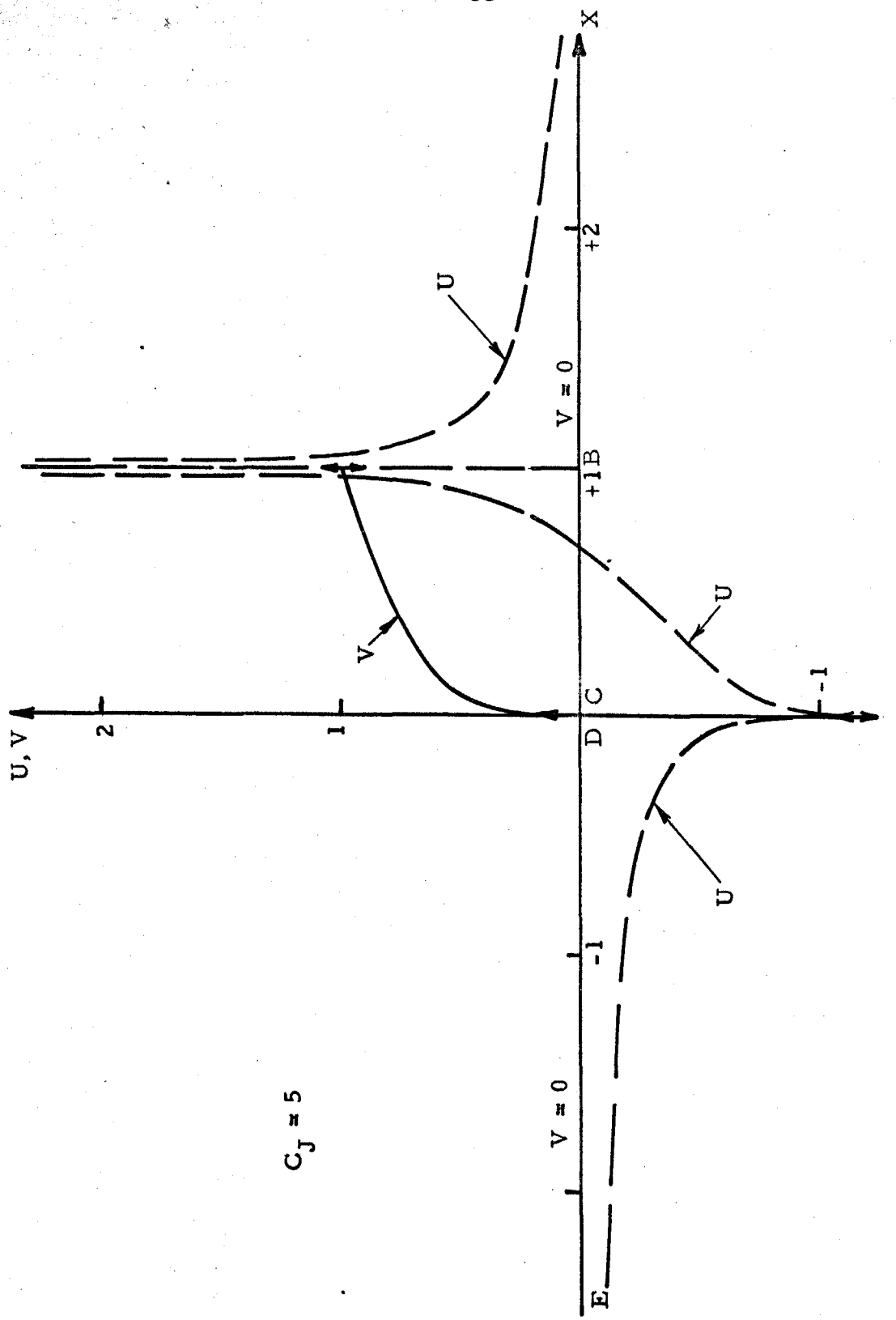

FIGURE 16: U AND V COMPONENT IN AUXILIARY PLANE

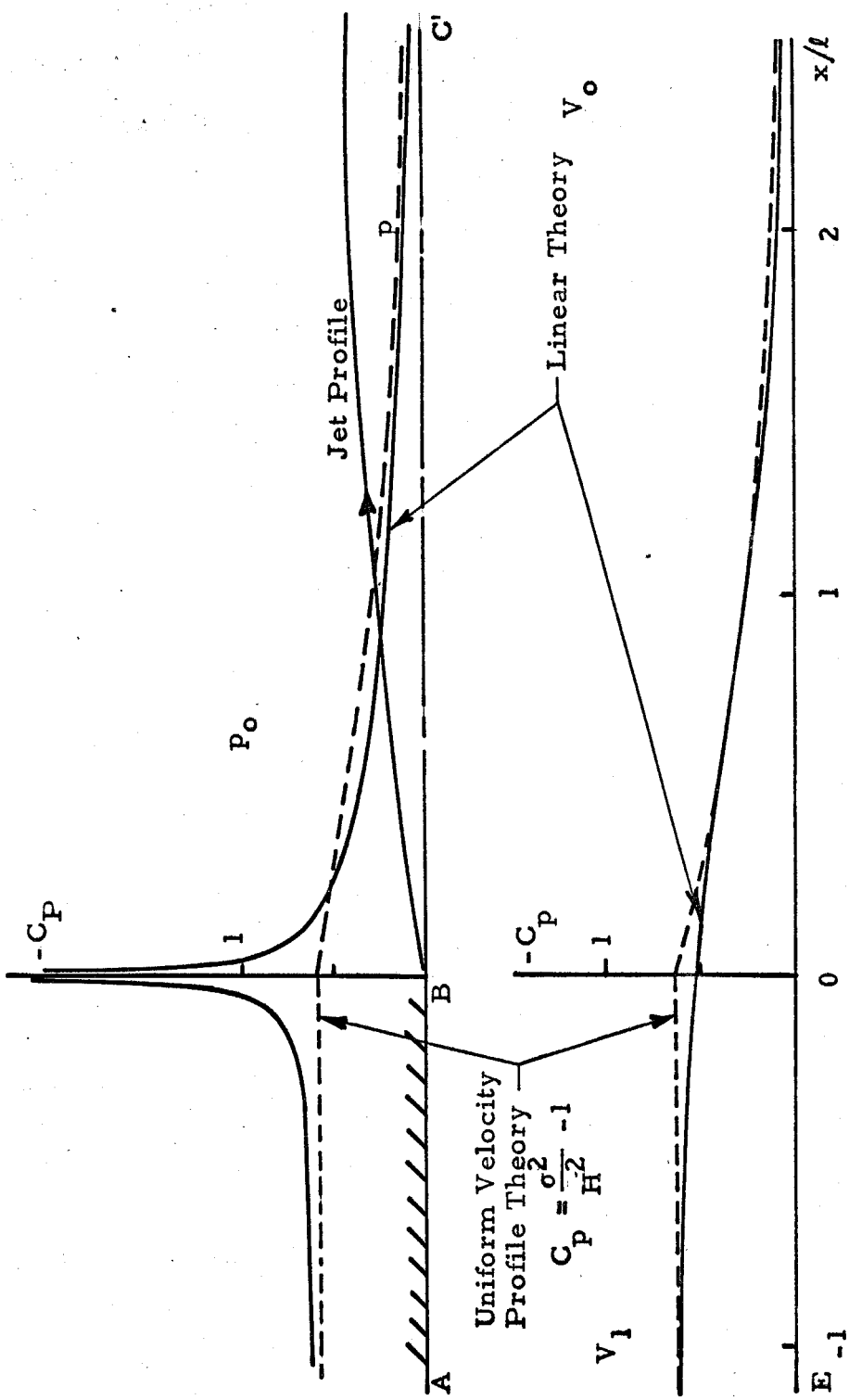

FIGURE 17: SOLUTION IN PHYSICAL PLANE

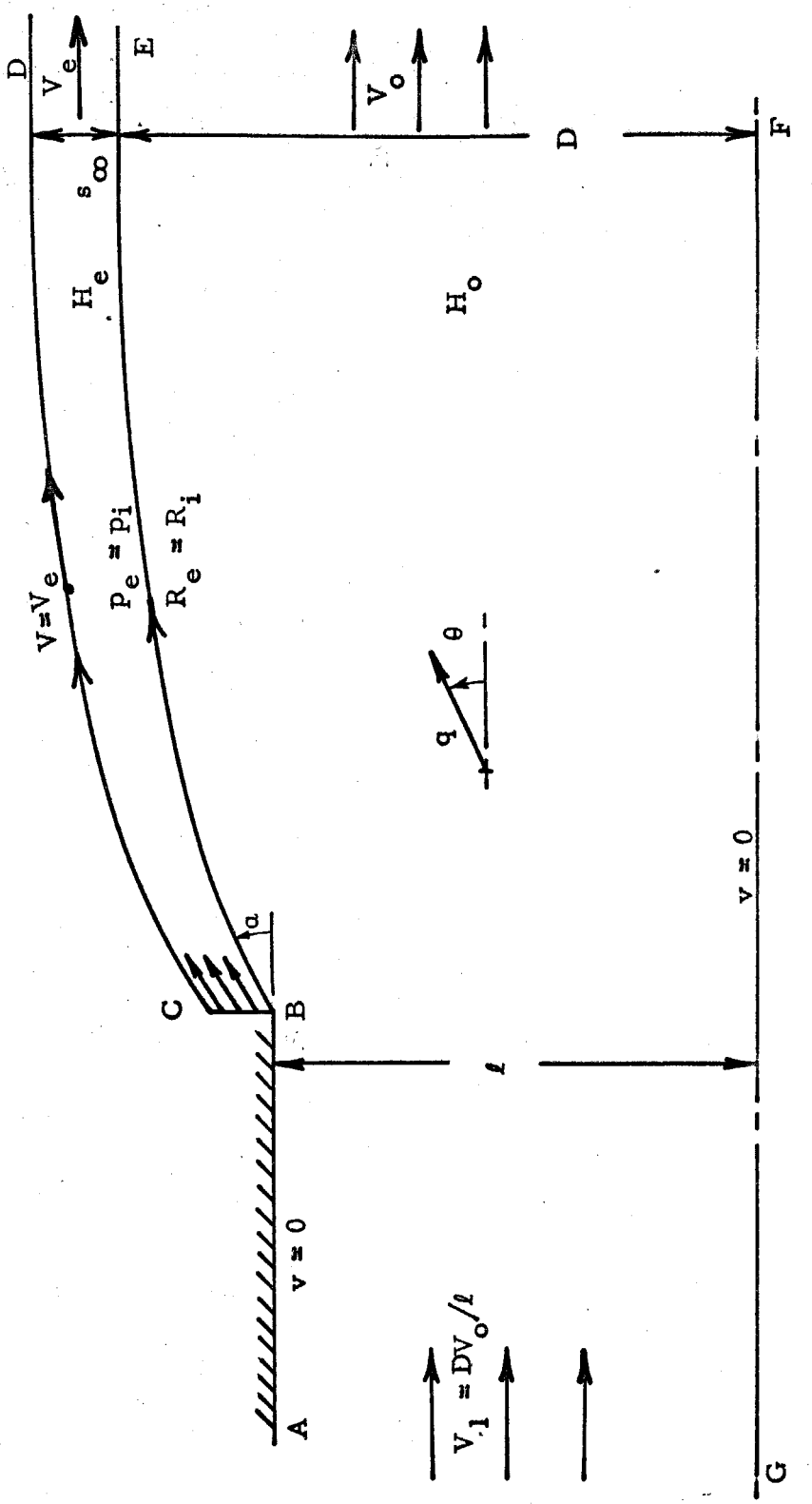

FIGURE 18: GEOMETRY OF NON-LINEAR PLANAR PROBLEM

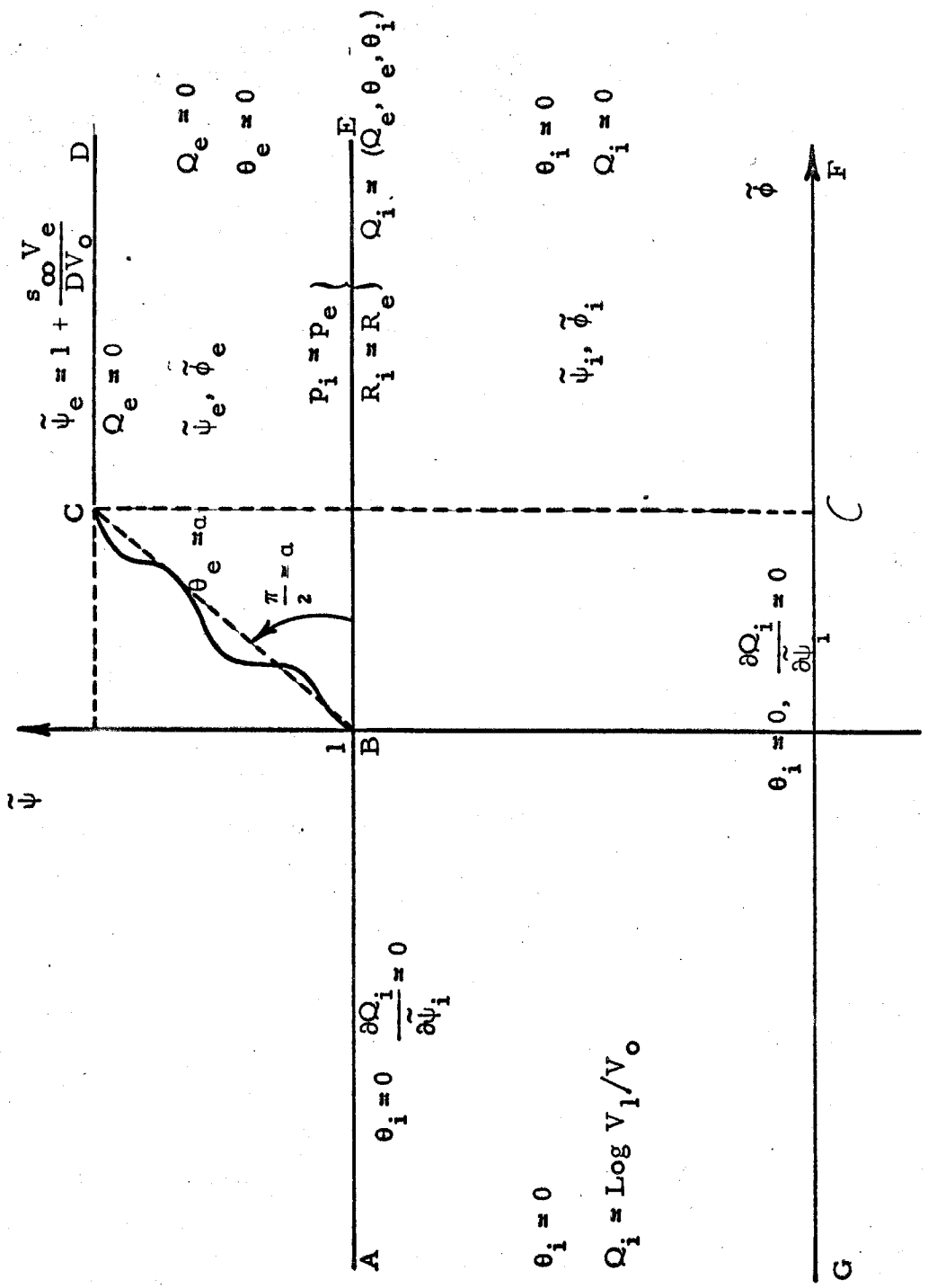

FIGURE 19: GEOMETRY IN THE POTENTIAL PLANE

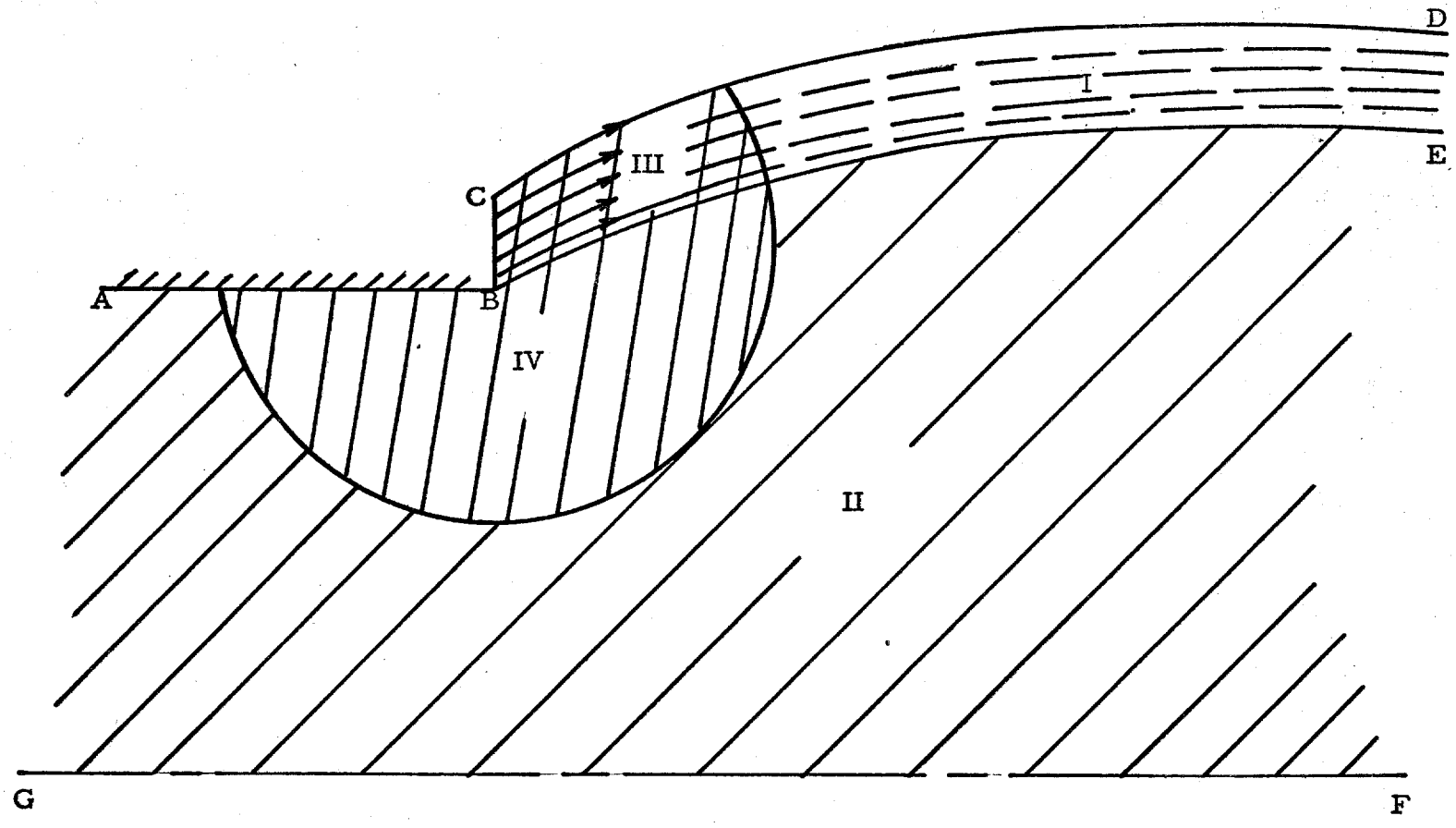

FIGURE 20: REGIONS OF THE NON-LINEAR PROBLEM

Inner Solution

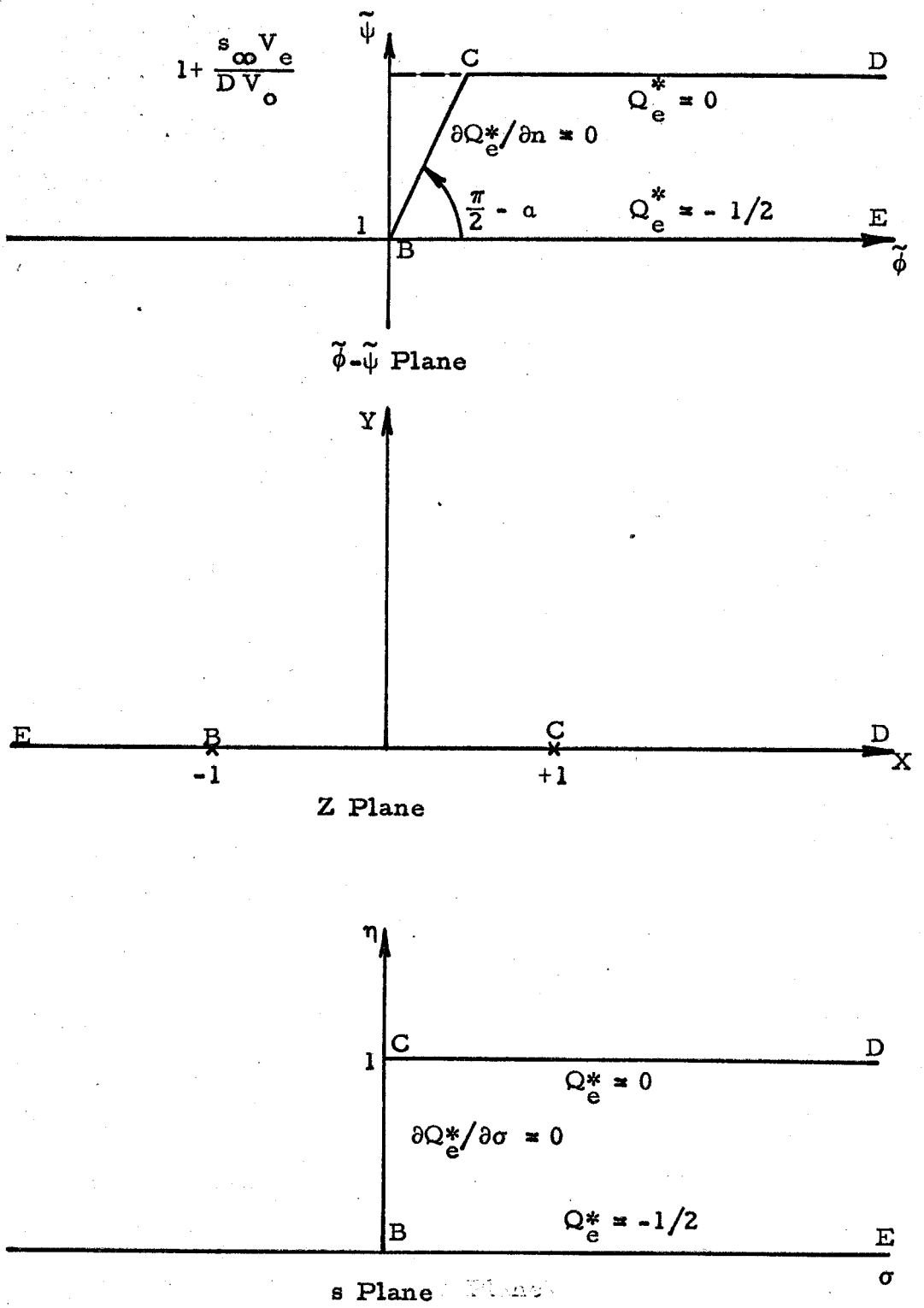

FIGURE 21: AUXILIARY PLANES FOR THE NON-LINEAR PROBLEM